Confidential – not for further distribution without written permission from GAMMA

GAMMA IPTA Processing Example Luxemburg

GAMMA Technical Report, Urs Wegmüller, 9-Nov-2005

Contents

1. Introduction

The purpose of this document is to describe an IPTA processing example. The input data to this example can be made available to GAMMA software users, so that they can experiment with a real IPTA processing case. The selected case is relatively simple as the test area covers mainly the city of Luxemburg. The selected test area is very small, which facilitates the provision of the input data and which makes testing more efficient. The selected test case is not particularly interesting as deformation in the selected area is minimal. Only ERS data are included in this processing. The integration of ASAR data into a combined ERS – ASAR IPTA processing is not the subject of this technical report but of a separate report.

Please notice that a relatively simple approach is used in the processing of the selected data set. The IPTA software offers a broad functionality which means that the processing can be done in very different ways. It is not the intention of this processing example description to provide a complete coverage of options available in the processing. It is also not intended to give the impression that the selected approach shall be the optimal one for the processing of this case. At some cases possible alternatives to the processing are mentioned.

The processing example refers to a very specific case. Specific file names and specific parameters (e.g. mli image width = 400 pixels) are used in the commands shown. The naming conventions used are such that it should be possible to identify which file is meant without providing lengthy definitions.

It is not the intension to describe every single step in the last detail.

2. Starting point

Two different "entry points" in the IPTA processing are supported. The first one is to start from the stack of co-registered SLC images. This starting point has the advantage that in includes the generation of a point target list (candidate list) and the conversion of SLC data from raster to the vector format. One disadvantage is that selecting a different point list than the one used by us may result in quite different problems along the processing, potentially requiring different processing solutions to solve the problem. To reduce this potential compatibility problem a pre-defined point candidate list and the related point SLC stack are also provided. So a "second" entry point is at the beginning of the analysis in the vector format representation.

In the following sub-sections the input data are further discussed. Only the stack of co-registered SLC and related SLC parameter files (Section 2.1) and the digital elevation model (Section 2.2) are basic input files. All other files can be derived from these or can be genuinely created (e.g. IPTA interferogram table which is the file containing the selection of interferometric pairs to be analyzed).

In Section 3 the IPTA processing steps in vector format start. It is rather recommended (at least for an initial reprocessing of this example) to use the vector data files which are provided, rather than new ones generated according to Section 2.7.

2.1 Stack of co-registered SLC and related SLC parameter files

The ERS RAW data were processed using the GAMMA MSP. An often used selection of processing parameters is that all the scenes (ERS) are processed to the same Doppler Centroid (or alternatively the bandwidth fraction in selected bandwidth can be selected, or alternatively each scene can be processed to its own optimal Doppler parameters).

Alternatively, ERS SLC data processed by an ESA Pac can be used.

One ERS SLC is selected as reference. Criteria used in the selection of this reference image, listed according to their importance, include:

- Doppler centroid near average Doppler Centroid of considered SAR acquisitions
- orbit near geometric center of orbital tube spanned by available SAR acquisitions
- low atmospheric distortions
- acquisition date near temporal average of available SAR acquisitions

For the first criterion every ERS-1 or ERS-2 scene except those acquired with significantly different Doppler parameters (i.e. many ERS-2 scenes in 2000 or later) qualifies.

For the second criterion a significant fraction of the available scenes qualifies if offsets up to about 200 m (for the perpendicular baseline component) are tolerated.

Among these scenes those with low atmospheric distortions should be identified. This is done by calculating 2D differential interferograms which include the scenes of interest. Of course, sufficient coherence and some idea on deformation signals present is required to be able to judge the presence of atmospheric distortions. Mainly pairs with short baselines and shorter time intervals are used for this purpose. A single "very flat" differential interferogram (Tandem pair, 35 day pair, 70 day pair) is a clear indication of low atmospheric distortions for both acquisitions of this pair.

The selection of a time near the temporal average of available SAR acquisitions is then used as an additional, but less important, criterion in the selection.

For the specific Luxemburg example the ERS scene acquired on 4-Nov-1999 (19991104) was identified as a good reference scene.

For this reference scene the SLC part covering the test area was extracted using the program SLC_copy. The extracted SLC section and the SLC parameter file for the extracted section are named 19991104.rslc and 19991104.rslc.par. Only for this *.rslc file the pixel scaling factors (range_scal_factor, azimuth_scale_factor) are exactly 1.00000). For all the other co-registered scenes the scaling values will be slightly vary from 1.0.

All the other SLC were co-registered to the reference SLC section using the programs offset_pwr and offset_fit. Typically, these programs were run twice to optimize the registration accuracy. The co-registration accuracy achieved is normally very good with standard deviations of the individual range and azimuth offset estimates from the offset regression fit of less than 0.2 pixels.

Alternatively, the novel programs (to be included in next GAMMA software distribution):

- rdc_trans
- SLC_interp_lt

can be used. The main purpose of these programs is to support the consideration of terrain height effects on the SLC resampling, which is somewhat relevant in the case of significant topography and long baselines. The first program calculates the transformation between the images based on the imaging geometry using SAR parameters (orbit, sensor, mode) as well as terrain heights (or an assumed constant terrain height). The transformation is stored in the form of a transformation lookup table. The second program supports the resampling using the second image to the reference geometry. The transformation lookup table can be refined based on the data itself in a similar way as used in the normal image co-registration (using offset_pwrm, offset_fitm for a rough but efficient refinement using multi-look intensity images and offset_pwr, offset_fit for a very accurate final refinement using the full resolution SLC data).

As a result of this step the ERS SLC (typically denoted .rslc) and the related SLC parameter files (.rslc.par) are available in the same geometry as the ERS reference SLC.

Important information in the SLC parameter files includes the orbit state vectors. Based on the orbit state vectors available in the SLC parameter files, respectively in the SLC parameter file stack, initial estimates of the interferometric baselines will be calculated. The use of the most accurate orbit state vectors available, e.g. PRC or DELFT state vectors, as supported in the GAMMA software strongly recommended. In the Luxemburg data example DELFT state vectors are used.

2.2 Digital elevation model (in map geometry)

When available an external DEM should be used in support of the IPTA analysis. To have at least an approximate idea of the local terrain height makes the IPTA more robust and more efficient. In many cases control points extracted from the DEM may also serve as absolute height reference. Furthermore, the DEM can be used for terrain corrected geocoding.

For the Luxemburg example we generated a DEM in UTM (Luxemburg.utm.dem) based on the 3-Arc-Seconds SRTM DEM. The exact map projection parameters used are defined in the DEM parameter file (Luxemburg.utm.dem_par). The size of this DEM is 840 x 760 pixels, at 10 meter pixel spacing. The heights indicated are heights above sea level (i.e. not WGS84 heights).

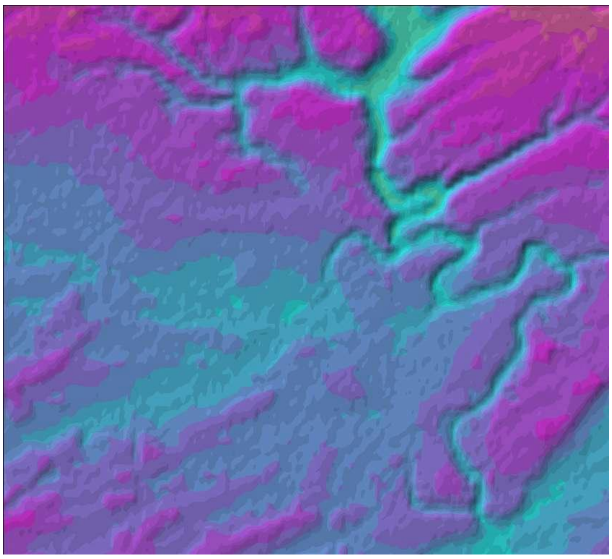

Luxemburg. Digital elevation model in UTM derived from SRTM 3” DEM.

2.3 Average multi-look intensity image in SAR geometry

An average multi-look intensity image is used as brightness for many displays. The average multi-look intensity image is calculated by first calculating for each registered SLC (*.rslc) the corresponding multi-look detected image (using the program multi_look). In the Luxemburg example this was done using 1 range and 5 azimuth looks. Then the average image is calculated. This is done by first generating the file rmli_list (which contains all the the individual *.rmli images. Then images with low quality or incomplete coverage can be removed from the list (by manual editing). Finally, the program ave_image is used to calculate the average image, a SUN rasterfile thereof is generated using ras_dB (or raspwr):

```
ls ../slc/*/*.rmli > rmli_list
e rmli_list
ave_image rmli_list 400 ave.rmli 1 - 1 1 1
ras_dB ave.rmli 400 1 0 1 1 -22. 3.5 0. ave.rmli.ras
```

In the Luxemburg example all the 56 *.rslc files could be used to generate the average intensity image ave.rmli.ras. Notice that the file 19991104.rmli.par contains the definition of the geometry of the average intensity image.

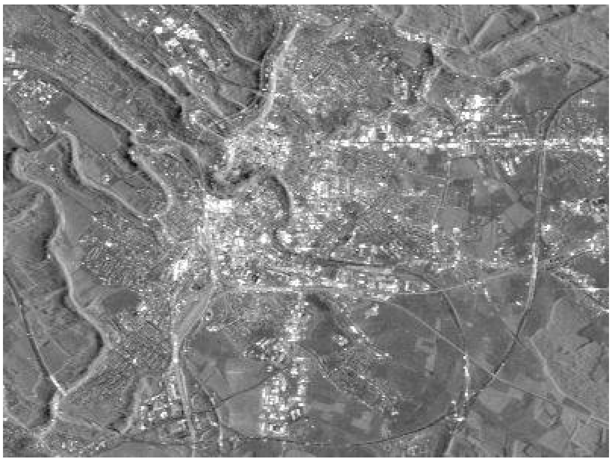

Average backscatter intensity image (in reference SAR geometry).

2.4 Refined geocoding lookup table, terrain height in SAR geometry, average multi-look intensity image in map geometry

Transformation between the selected map geometry (in the Luxemburg example UTM) and the SAR (slant range) geometry and vise-versa is relevant for example to calculate a height reference in the SAR geometry or to transform the results from SAR geometry to map geometry. In the GAMMA software this is done using a geocoding lookup table and a refinement of this transformation using an automated matching between images representing the different geometries.

A possible sequence to determine the refined geocoding lookup is the following:

```
cp Luxemburg.utm.dem_par Luxemburg.utm.dem_par.tmp
```

gc_map 19991104.rmli.par - Luxemburg.utm.dem_par Luxemburg.utm.dem
    Luxemburg.utm.dem_par.tmp - 19991104.lt 1 1 19991104.sim
geocode 19991104.lt 19991104.sim 840 19991104.sar_sim 400 300 0 0
create_diff_par 19991104.rmli.par - 19991104.diff_par 1
offset_pwrm 19991104.sar_sim 19991104.rmli 19991104.diff_par 19991104.offs
    19991104.snr 128 128 offsets 2 12 12 7.0
offset_fitm 19991104.offs 19991104.snr 19991104.diff_par coffs coffsets 7.0 1
offset_pwrm 19991104.sar_sim 19991104.rmli 19991104.diff_par 19991104.offs
    19991104.snr 128 128 offsets 4 24 24 7.0
offset_fitm 19991104.offs 19991104.snr 19991104.diff_par coffs coffsets 7.0 1

For this small section only a constant range and azimuth offset (offset polynomial with only 1 parameter) is determined. The final model fit standard deviation is 0.22 pixel (mli pixel) in slant range and 0.038 azimuth pixel (5-look mli pixel).

The refined lookup table for reference section is calculated using:

gc_map_fine 19991104.lt 840 19991104.diff_par 19991104.lt_fine 1

Based on this refined lookup table the average SAR intensity image can be transformed to the map geometry:

geocode_back ave.rmli 400 19991104.lt_fine ave.utm.rmli 840 760 2 0
dispwr ave.utm.rmli 840

and the DEM can be transformed to the mli SAR geometry to serve later on as height reference in the IPTA processing:

geocode 19991104.lt_fine Luxemburg.utm.dem 840 19991104.hgt 400 300 0 0
dishgt 19991104.hgt 19991104.rmli 400 1 1 0 256. 1. .4

The refined geocoding lookup table, 19991104.lt_fine, the geocoded average intensity image, ave.utm.rmli, and the heights in SAR geometry, 19991104.hgt are included with the input data for the Luxemburg example.

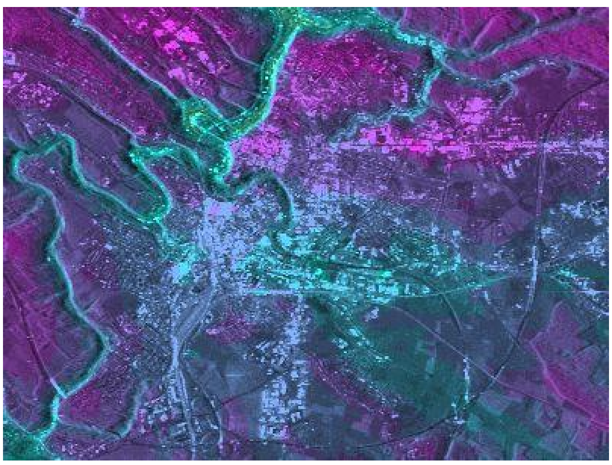

Average backscatter intensity image SRTM 3” DEM based heights (color scale) in

(geocoded, i.e. transformed to map geometry).	SAR geometry (with average backscattering used as image brightness).

Notice, that the SRTM heights are geoidal heights (i.e. the height Datum differs from the horizontal Datum). When interpreted as WGS84 heights this means that there is an offset corresponding to the difference between the local geoid and the WGS84 ellipsoid. In the initial lookup table calculation this height offset results in up to a couple of pixels range and azimuth offset. Nevertheless, such offsets are identified and compensated in the refinement. No additional geocoding errors should arise from the use of the different height Datum.

2.5 IPTA SLC table (SLC_tab)

The SLC_tab contains the filenames of the registered SLC and the corresponding SLC parameter file. The 56 lines of the SLC tab for the Luxemburg example may look similar to:

/m/Luxemburg/slc/19920420/19920420.rslc /m/Luxemburg/slc/19920420/19920420.rslc.par
/m/Luxemburg/slc/19920525/19920525.rslc /m/Luxemburg/slc/19920525/19920525.rslc.par
/m/Luxemburg/slc/19920803/19920803.rslc /m/Luxemburg/slc/19920803/19920803.rslc.par
...
/m/Luxemburg/slc/20030102/20030102.rslc /m/Luxemburg/slc/20030102/20030102.rslc.par
...

Line 47 contains the reference SLC. The editing of the SLC_tab is manually. For the Luxemburg example an SLC_tab is included but it is necessary to modify the path.

2.6 IPTA interferogram table (itab)

The itab contains the definitions of the pairs used in the IPTA processing. In the simplest case with a single ERS reference the itab may look similar to:

47 1 1 1
47 2 2 1
47 3 3 1
...
47 47 47 1
...
47 56 56 1

The first column contains the reference SLC number, the second column the slave SLC number, the third column the number of the pair and the forth column a flag indicating if a pair is activated (1) or not (0).

Notice, that the auto-interferogram (47 47 47 1) of the reference scene is included. This is highly recommended as the atmosphere for the reference scene will be in this record later on in the processing.

Using a single reference scene is an adequate choice for a case with a very high number of scenes available. Alternative choices are preferred for sets of fewer scenes (e.g. each possible combination).

The itab for a single reference (SLC 47) is included in the input data files. The editing of the SLC_tab is manually.

2.7 Point list (pt)

A key element of the IPTA is that the interferometric analysis is only done for selected points. The point list plays an essential role in this, as it contains the selected point definitions. Each point is defined by its range and azimuth coordinates. These coordinates are integer pixel numbers relative to the reference SLC geometry. An important reason for the selection of points with point target like scattering characteristics is the low geometric decorrelation of these targets which permits to include even interferometric pairs with baselines above the critical one in the analysis.

In the Luxemburg example, two different approaches were used to select the candidate points. The first approach is based on the individual co-registered SLC the IPTA programs to identify point targets based on their special spectral characteristics. The second approach is based on the idea that point targets do not show the speckle behavior associated with distributed targets since, by definition, a single coherent scatterer dominates the echo. One consequence is that a significantly lower temporal variability is observed for point targets as compared to distributed targets. For large SLC data stacks this characteristic can be used to identify point target candidates.

2.7.1 Generation of point target candidate list based on spectral properties of individual SLC

Well focused, dominating point targets have a characteristic spectral behavior which differs from that of distributed targets. The IPTA program sp_stat permits to identify point targets based on low spectral phase diversity. This is done for individual SLCs. As an additional criterion dominant backscattering (i.e. backscattering above a threshold) can be used. sp_stat generates a point target candidate list based on a single SLC. Considering, that multiple SLC are available it is recommended to repeat this procedure for several SLC or even for every available SLC. Either the point lists obtained are combined, or as was used in the Luxemburg example, the spectral characteristics are averaged over the stack of SLC and then the average spectral behavior is used to determine the candidate points. This is done using the following steps. In a first step sp_stat is executed for each of the co-registered SLC:

sp_stat <data>.rslc - <data>.cc <data>.msr <data>.pt 400 0.0 0.4 1.0 4 4 - - - - - - 1

Then average cc and msr files are calculated using:

ls *.cc > cc_list
ave_image cc_list 400 cc_ave
ls *.msr > msr_list
ave_image msr_list 400 msr_ave

The average cc_ave and msr_ave are then used to derive a candidate point list:

single_class_mapping 2 ave.sp_cc 0.35 1.0 ave.sp_msr 1. 100. pt2map.ras 400 1 0 1 1
image2pt pt2map.ras 400 pt1 1 1 6

The result is a point list with 9317 candidates (file pt1).

2.7.2 Generation of point target candidate list based on a low intensity variability

Point targets do not show the speckle behavior associated with distributed targets since, by definition, a single coherent scatterer dominates the echo. One consequence is that a significantly lower temporal variability is observed for point targets as compared to distributed targets. This characteristic is used to identify point target candidates in large SLC data stacks (program pwr_stat). Pre-conditions for the use of this method are 1) well focused SLC data, 2) an accurate co-registration of the SLC and 3) an accurate radiometric calibration. As measure for the temporal variability the mean/sigma ratio (where mean is the temporal average of the backscattering and sigma is the standard deviation of the backscattering from this average) is used. For fully developed speckle a mean/sigma ratio of 1.0 is expected. Even smaller values can be observed if the variability is not just caused by speckle but also by temporal change. In the case of a stable point target a value significantly above 1.0 is expected. Candidates are selected by setting a lower threshold (e.g. 1.5) for the mean/sigma ratio.

As an additional criterion backscattering above an indicated threshold can be used (program pwr_stat). This criteria is related to the condition that the point target does not only need to be present, but it has to dominate the clutter scattering. The threshold is indicated by a factor to be multiplied with the spatial average of the backscattering. A factor 1.0 means that the backscattering has to be above the spatial average. This second condition permits to avoid selection of many point target candidates in low backscattering areas such as radar shadow.

In the Luxemburg example we used the command:

```
pwr_stat SLC_tab 19991104.rslc.par MSR pt2 1.4 0.5 - - - - 1 1
```

A mean to sigma ratio (MSR) threshold of 1.4 was used in combination with the requirement that the backscattering is above 0.5 * the spatial average. A relative normalization of the backscattering (based on the image averages) was selected.

The result is a point list with 8760 candidates (file pt2). The temporal variability criterion works quite well for large stacks (> 25 images). For smaller stacks it becomes less reliable. Therefore, other criteria are included in the IPTA for this case.

2.7.3 Merging of point target candidate lists

The two point lists determined are then combined into a single point list. This is done using the program merge_pt. Different logical operations can be used. In the Luxemburg example we used “or”, i.e. a point is included in the combined list if it fulfills either the spectral criterion (pt1) or the power variability criterion (pt2):

```
echo "pt1" > plist_tab
echo "pt2"  >> plist_tab
merge_pt plist_tab pt 1 0 0
```

The combined list pt contains 14190 points.

The point lists can be visualized using:

ras_pt pt - ave.rmli.ras pt.ras 1 5 255 0 0 3

Below the point lists derived using the two criteria and the combined point list are shown.

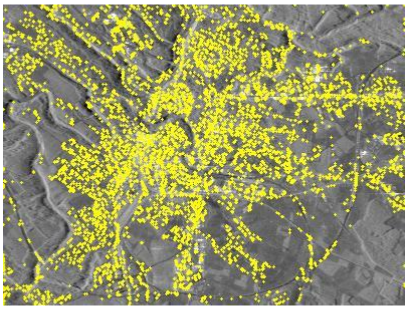

Spectral diversity based candidate list

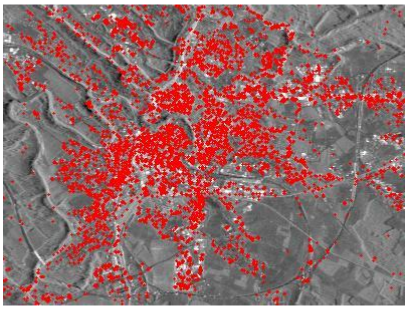

Power variability based candidate list

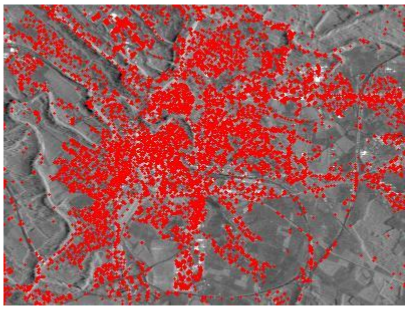

Combined candidate list

The presence of point targets depends strongly on the scene. Many point targets are typically present in built-up areas. Very few point targets may be present in other areas.

It is also important to remember that at this stage only candidates are selected. At a later stage of the processing the quality of the candidates will be more carefully evaluated, respectively candidates of poor quality will be excluded.

The reliability of the point target candidate selection will depending on 1) the number of SLC in the stack, 2) the quality of the processing (focusing, registration, calibration), and 3) the thresholds applied.

The combined point list pt is included in the Luxemburg example input data set. To have a high compatibility between your own processing and the discussion provided in this document it is recommended that the provided point list is used. The point list provided is in no way considered the optimal one, but only as one reasonable selection.

2.8 SLC point data stack (pSLC_par, pSLC)

For the points of the candidate list the SLC values are extracted and written in the vector data SLC point data stack. Apart from the SLC point data stack a stack of the related SLC parameter files is generated (to have easy access to it). This is done using the program SLC2pt:

SLC2pt SLC_tab pt - pSLC_par pSLC –

Notice that the size of this stack (56 x 14190 x 4 = 3.17856 MByte) is much reduced as compared to the size of all the registered SLC (56 x 400 x 1500 x 4 = 134.4 Mbyte). The actual size of the SLC point data stack provided is somewhat larger as it also contains additional records for 10 co-registered ASAR scenes.

2.9 Baselines (pbase)

The baseline file, pbase contains all the individual baseline files (*.base) of the interferometric pairs selected in the itab file. The baseline file including the orbit based initial baseline estimates is generated using:

base_orbit_pt pSLC_par itab - pbase

To display the baselines the following command can be used:

base_par_pt - pbase - 0

The quality of these baseline estimates depends on the quality of the orbits used (highly recommended are PRC or DEFLT orbits).

To make a plot of the perpendicular baseline components the script base_calc is used:
base_calc SLC_tab 19991104.rslc.par bperp_plot.xmgrace bperp.ascii itab.tmp 0 - - -

Notice that this script also generates a new itab (itab.tmp is indicated here not to overwrite the previously determined itab).

The plot is then made using XMGRACE:
xmgrace bperp_plot.xmgrace

Notice that using 365.24805 days as tick interval for X axis provides annual intervals in the tick labels. The plot is then printed and may look as follows:

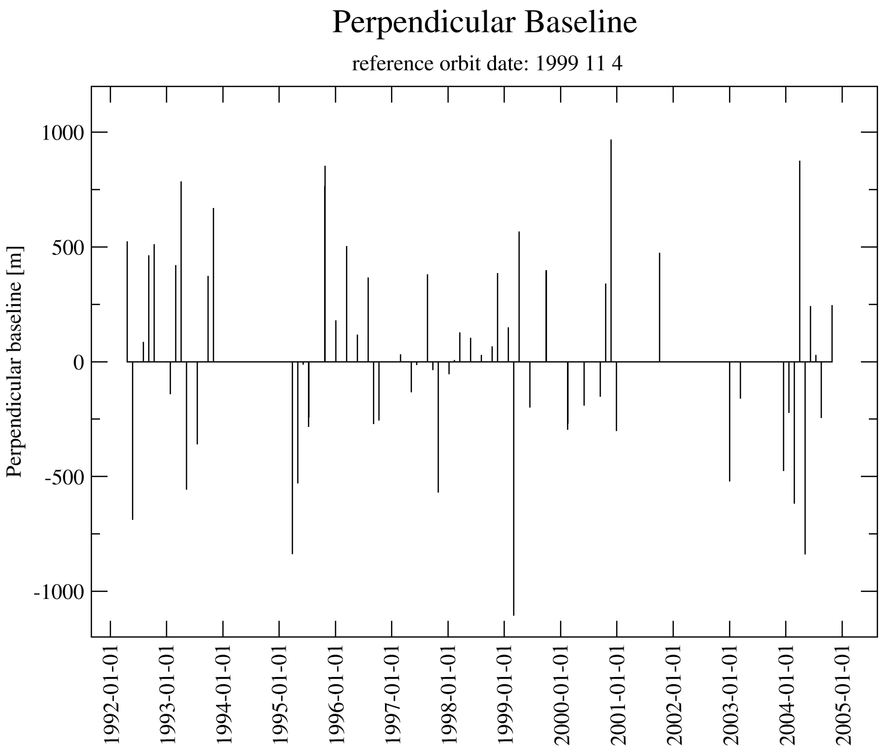

Perpendicular baseline components relative to the selected reference orbit 4-Nov-1999. (In this plot the baselines for the available ASAR data are also shown).

2.10 Input files

At this stage the following files are available:

Co-registered ERS SLC data (and related files):

In sub-directory slc/<date>
<date>*.rslc,* <date>*.rslc.par, p*<date>.slc.par
<date>*.rmli,* <date>*.rmli.par,* <date>*.rmli.jpg (quicklook)*

2D data files in map geometry (and related parameter files):
Luxemburg.utm.dem, Luxemburg.utm.dem_par
19991104.lt_fine, 19991104.diff_par
ave.utm.rmli, ave.utm.rmli.ras

2D data files in SAR geometry:
19991104.rslc.par (2D SLC files are not included in this list)
ave.rmli, ave.rmli.ras , 19991104.rmli.par
19991104.hgt

Vector point data files and stacks:
pt
pSLC

IPTA files:
SLC_tab
itab
pSLC_par
pbase

Other files:
bperp.ascii, bperp_plot.gif

All these files are provided for the Luxemburg example.

3. Generate initial differential interferograms

3.1 Generate DEM point data file (pdem)

The DEM point data file is simply generated by extracting the DEM height values at the point locations:

data2pt 19991104.hgt 19991104.rmli.par pt 19991104.rslc.par pdem 1 2

The point heights can be displayed (in 2D) using:
pdisdt_pwr24 pt - 19991104.rslc.par pdem 1 19991104.rmli.par ave.rmli 256. 1

3.2 Generate interferogram point data stack (pint)

Next the interferogram point data stack is calculated using the command:

intf_pt pt - itab - pSLC pint 1

The layers of pint can be displayed using pdismph_pwr24 using:
pdismph_pwr24 pt - 19991104.rslc.par pint 25 19991104.rmli.par ave.rmli 1

Notice, that these interferograms include the orbital fringes (many for the larger baselines).

3.3 Calculate and subtract phase model (psim_unw0)

Next, the phase model point data stack is calculated based on:

- the SLC point data stack
- the SLC parameter stack
- the itab
- the baseline estimates based on the orbits
- the point DEM heights

using the command:

phase_sim_pt pt - pSLC_par - itab - pbase pdem psim_unw0 - 0 0

No deformation and no atmospheric phase is considered in this initial phase model. Furthermore, initial and not refined baselines are used. The simulated (unwrapped) phases are subtracted from the complex valued point interferograms to get the point differential interferograms (complex values):

sub_phase_pt pt - pint - psim_unw0 pdiff0 1 0

The resulting 56 initial differential interferograms can be visualized using:

prasmph_pwr24 pt - 19991104.rslc.par pdiff0 - 19991104.rmli.par ave.rmli 1

and show the following:

For pairs with relatively short baselines the differential interferometric phase looks already relatively smooth. An interpretation (requiring also phase unwrapping) appears feasible.

For pairs with large baselines the phase looks very noisy. Examples for a short and a long baseline are shown below.

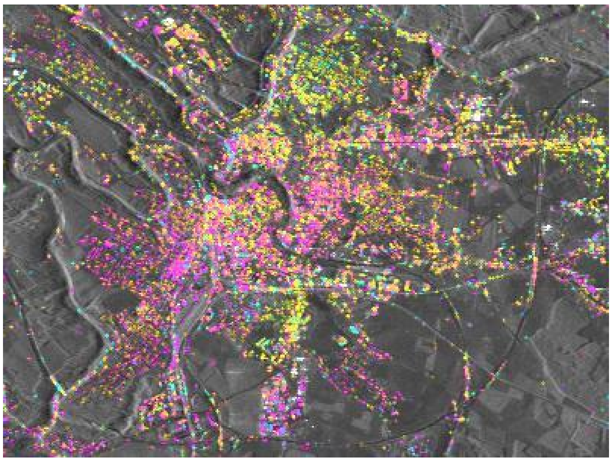

Initial differential point interferogram for short baseline pair (pair 22, $B_{\perp}$ 115m).

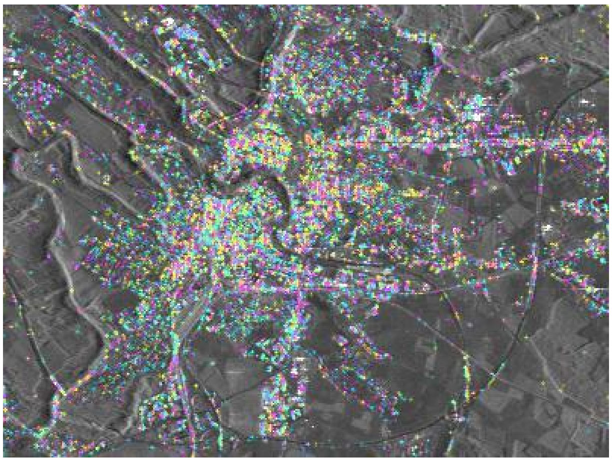

Initial differential point interferogram for long baseline pair (pair 32, $B_{\perp}$ -567m).

Considering the high spatial phase noise of the long baseline point differential interferogram it is not clear if the differential interferometric phase may be interpreted. At this large baseline the sensitivity of the interferometric phase to terrain height is quite high. Even residual height errors of a several meters result a noisy appearance of the differential interferogram.

Apart from the smoothness of the differential interferometric phase it is also possible to check the quality of the initial baselines (only for those pairs which look relatively smooth). A few pairs, e.g. 15 and 48 show a distinct range phase trend which is most probably related to errors in the baseline model used.

Other differential interferograms appear relatively coherent, but show spatial variations of the differential interferometric phase which deviate significantly from that of other pairs covering a similar time interval, which is a clear indication of atmospheric distortions affecting this pair.

Examples of pairs with obvious baseline errors and atmospheric distortion are shown below.

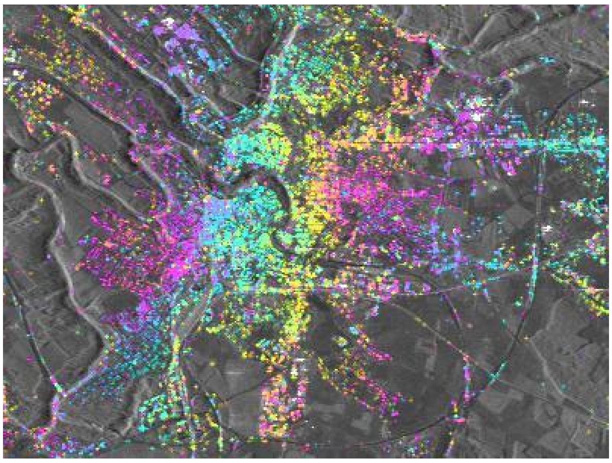

Initial differential point interferogram for short baseline pair (pair 15, $B_{\perp}$ -10m).

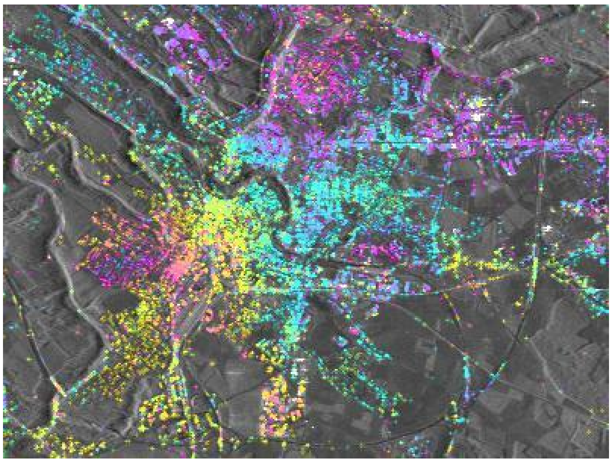

Initial differential point interferogram for long baseline pair (pair 37, $B_{\perp}$ 26m).

4. Phase regression analysis for pairs of points

4.1. Introduction to the phase regression analysis

The analysis of the differential interferometric phases in the time direction is an important element of an interferometric point target analysis. More specifically, spatial differences of the differential interferometric phases (between pairs of point targets) are analyzed. For a stack of 56 records (as in the Luxemburg example) this means that 56 spatial differences between differential interferometric phases are considered.

The interferometric phase model indicates a linear dependence of the topographic phase on the perpendicular baseline component with the slope of the regression indicating a relative height correction. This height correction is the height which needs to be added to the second point, so that its phase becomes consistent with that of the reference point.

Furthermore, the phase model indicates a linear time dependence for deformation rates which differ between the second point and the reference point. So the regression is further improved and made more robust by also considering a linear phase dependence with time, which is equivalent to a constant relative deformation rate.

A two-dimensional regression analysis is done with the dimensions corresponding to the perpendicular baseline (of the interferometric pairs) and to the time difference (between the two SLC of the interferometric pairs). The related slopes correspond to relative terrain height corrections and relative linear deformation rates.

For complex valued differential interferograms one problem of the regression is that the phases are still wrapped. For large stacks performing a two dimensional linear regression using the wrapped phase data is possible. In this case one part of the optimization is to find the correct phase ambiguities. For small stacks spatial phase unwrapping may be required prior to the regression step (this is supported by the program mcf_pt using a phase unwrapping algorithm based on Minimum Cost Flow optimization techniques applied to a triangular irregular network).

The phase differences will of course not match perfectly with the two-dimensional regression. The phase standard deviation includes terms related to phase noise (ϕ_{noise}), atmospheric path delay related phase (ϕ_{atm}), deformation phase (ϕ_{def}), and baseline error related phase. Except for ϕ_{noise}, these terms depend all on the distance between the two points. Consequently, for pairs with short spatial separation this regression analysis can be done independently of the quality of ϕ_{atm}, ϕ_{def}, and the baseline. The standard deviation of the phase from the regression is used as a quality measure, permitting for example to detect and reject points which are not suited for IPTA analysis.

4.2. Interactive point-wise phase regression analysis (dis_ipta)

Such a regression analysis can be done interactively, using the program dis_ipta. A reference point is selected wit a right mouse click, a second point is selected using a left mouse click. For the selected point pair the regression and the individual (now unwrapped) differential interferometric phases are shown. Values as the height correction, the linear deformation rate, and the phase standard deviation from the fit are printed to the screen:

dis_ipta pt - pSLC_par - itab pbase 0 pdiff0 1 pdiff0.22.ras 30 0.01 2

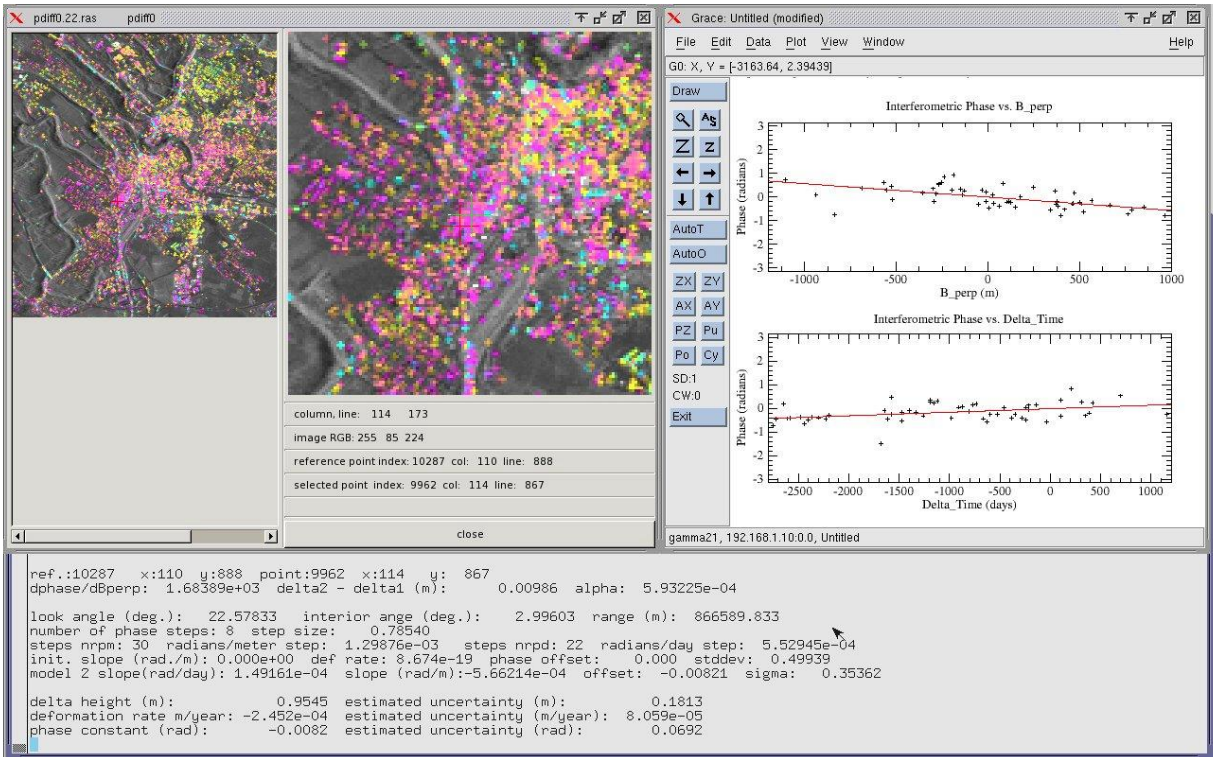

Example of IPTA regression analysis for a pair of points. In the upper right corner the two-dimensional phase regression plot is shown for a case with a small relative height correction. In the upper plot the baseline dependence of the phase difference is shown after compensation of the time dependence and in the lower plot the time dependence after compensation of the baseline dependence.

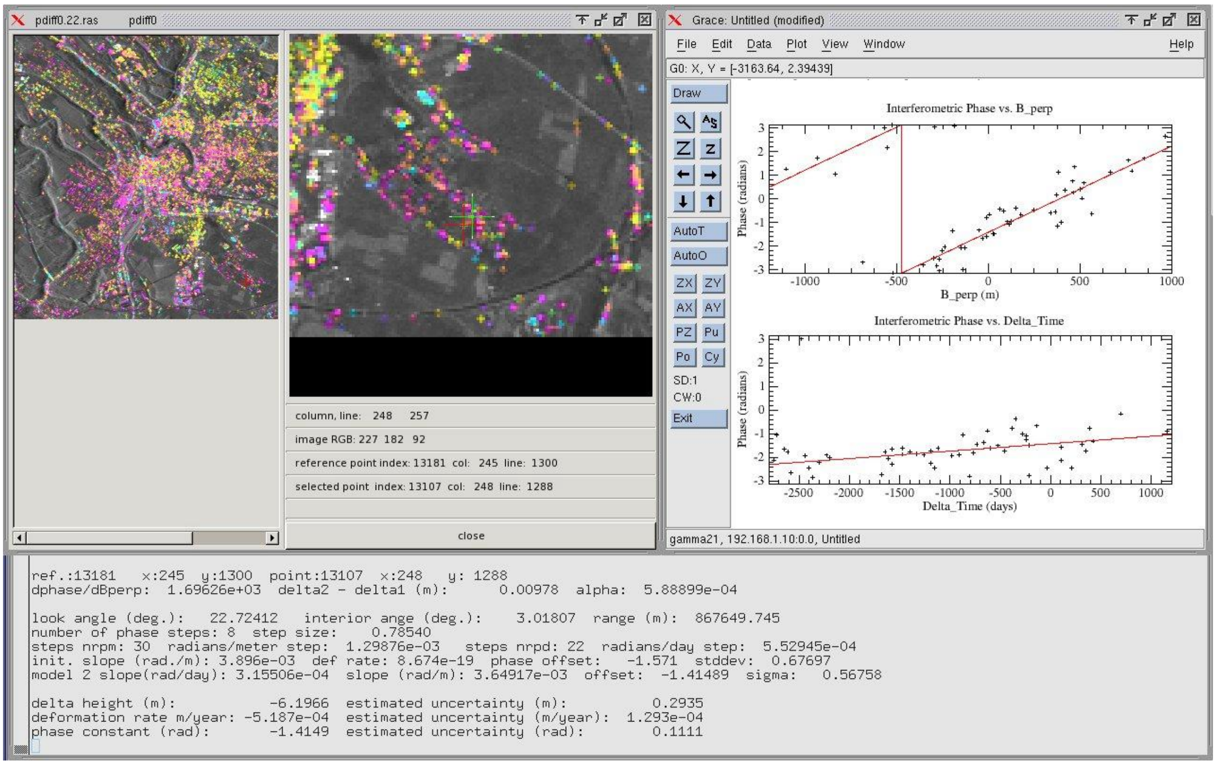

Example of IPTA regression analysis for a pair of points. In the upper right corner the two-dimensional phase regression plot is shown for a case with an intermediate relative height correction. Unwrapping of the phase differences was done successfully as part of the regression analysis. For the display the unwrapped phases were re-wrapped.

4.3. Automated phase regression analysis (multi_def_pt, def_mod_pt)

For the processing of the entire data set the same type of analysis is done in an automated manner using one of the programs multi_def_pt or def_mod_pt. The central algorithm used in these programs is identical. What is different is to what point pairs it is applied. In dis_ipta it is applied to operator selected pairs, in def_mod_pt to all points of the point list with one reference point, and in multi_def_pt to all points of the point list with one global reference point and a patch-wise local reference point.

In the case of an original differential interferogram stack the regression can only be determined reliably for point pairs which are relatively close (in distance) to each other. With increasing distance between the two pairs phase components as the atmospheric distortion, baseline error related residual orbital phase trends, and higher relative deformation rates result in higher deviations of the individual points from the regression plane. At a certain "noise level" the regression can no longer be solved reliably for the available wrapped phases.

The program multi_def_pt addresses this difficulty by using multiple patches. Within each patch one reference is determined. For each other point in the patch the regression analysis is performed using the patch reference as reference. In addition, regression analyses are conducted between the patch references.

So the next step in the IPTA processing is to run multi_def_pt for the initial differential interferogram. A reference point number has to be indicated for this step. The reference should be a high quality point, typically in a stable area, but not far from the main areas of interest. It can be determined interactively using dis_ipta. In the Luxemburg example we selected point number 7436. multi_def_pt is run with the following parameters:

multi_def_pt pt - pSLC_par - itab pbase 0 pdiff0 1 7436 pres1 pdh1 pddef1 punw1 psigma1 pmask1 30. 0.01 100 1.2 1.0 2 0 500

The choice of the parameters has a strong effect on the execution time of the program and on the result achieved.

To select a maximum height correction of 30 m is based on our experience that corrections found are typically smaller than this. In addition, allowing a higher maximum height correction would further reduce the efficiency and might result in more phase unwrapping errors.

To select 0.01 m/year maximum deformation rate is also based on experience. Somewhat higher values may be selected in cases with stronger deformation. Nevertheless, the chances to get a result with unwrapping errors also increases. Notice that this value is not the maximum for the absolute deformation rate, but only for the relative rate between the point pairs. In spite of this maximum higher rates may be detected.

A patch size of 100 range pixels, a maximum phase standard deviation between pairs within a patch of 1.2 radian, and a maximum phase standard deviation of 1.0 radian between patch references turned out to be a reasonable choice for this example.

Furthermore, this first regression analysis was restricted to pairs with baselines $B_{\perp} < 500$m.

The results from the regression analysis include:

- height corrections (pdh1),
- linear deformation rate corrections (respectively a first estimate, pddef1),
- point quality measures (phase standard deviation from regression fit, psigma1),
- residual phases (deviation from regression fit, pres1) for each record
- unwrapped interferometric phase (punw1) for each record of interferogram stack .

These different point data sets and stacks can be displayed using commands as:

```
pdisdt_pwr24 pt pmask1 19991104.rslc.par pdh1     1 19991104.rmli.par ave.rmli 30.0 1
pdisdt_pwr24 pt pmask1 19991104.rslc.par pddef1   1 19991104.rmli.par ave.rmli 0.01 1
pdisdt_pwr24 pt pmask1 19991104.rslc.par psigma1  1 19991104.rmli.par ave.rmli 1.5 1
prasdt_pwr24 pt pmask1 19991104.rslc.par pres1    - 19991104.rmli.par ave.rmli 12.6 1
```

The number of “accepted” points with sigma < sigma_max = 1.200 : 12190

4.4. Detecting patch related phase unwrapping errors

An important step between the differential interferogram stack (pdiff0) and the outputs of the regression analysis is the phase unwrapping of the differential interferometric phase. Using multi_def_pt this phase unwrapping is done in the temporal dimension (i.e. through the stack). At this stage the modeled phase may deviate quite significantly from the observed (wrapped) one – only a linear deformation rate is accounted for, there may be strong atmospheric distortions, there may be baseline errors. As a consequence it cannot be expected that the phase unwrapping will be correct for all points and all layers. Some phase unwrapping errors are very obvious in the spatial dimension when displaying the residual phase.

Examples of a residual phase image which looks "correct" (i.e. it is not likely that the unwrapping of the related differential interferogram will contain errors) and one which clearly indicates phase unwrapping errors are shown below. To make such phase errors obvious a scaling of 2 or 3 phase cycles per color cycle is used in pdisdt_pwr24 or prasdt_pwr24 (with one phase cycle per color cycle the unwrapping errors are not visible).

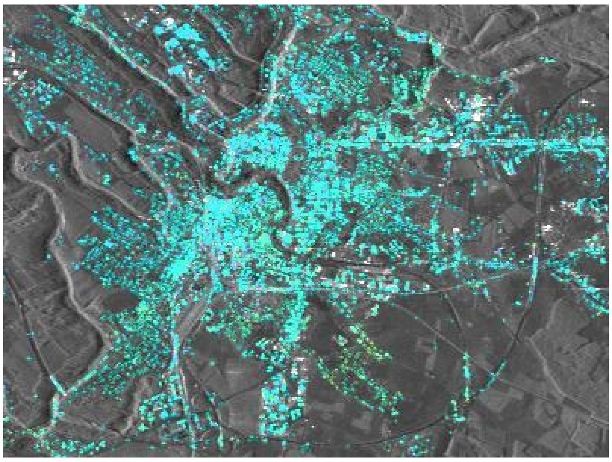

Residual phase (pres1) point image which looks "correct" (pair 7, $B_\perp$ 418m).

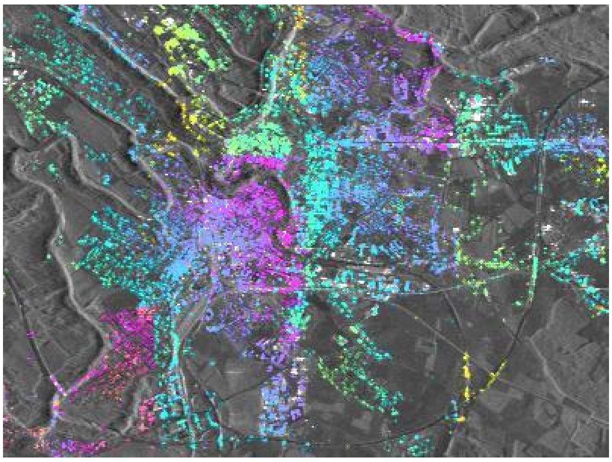

Residual phase (pres1) point image which clearly indicates phase unwrapping errors (pair 23, $B_\perp$ 364m).

Furthermore, there are some layers (pairs) without residual phases as they were excluded from the regression analysis by the "baseline shorter than 500m" criteria used in multi_def_pt.

Of course incorrectly unwrapped phases will result in additional errors in the parameters estimated in the regression analysis. To avoid the influence of incorrect unwrapping all those layers with correct unwrapping are identified and then used to re-estimate point height corrections and an initial linear deformation rate.

The layers with correct unwrapping are identified as those layers for which the residual phase does not show indications for phase unwrapping errors – this is done by checking each of the residual phase images generated by prasdt_pwr24.

4.5. Re-running regression analysis for correctly unwrapped layers

In the Luxemburg example the correctly unwrapped layers are the following:

4,6,7,10,11,16,20,22,25,26,27,28,30,31,33,34,35,36,39,40,44,46,47,49,50,51,52,54,55,

The itab is copied to a new name and the flags of all pairs without correct unwrapping are set to 0 (manual editing):

cp itab itab.selection1
nedit itab.selection1 &

Instead of re-running multi_def_pt for these layers (which would include again the unwrapping) and which would include again the possibility of errors in the parameter estimation related to the multi-patches approach used the program def_mod_pt and the (correctly) unwrapped phases (punw1) are used to re-run the regression analysis:

def_mod_pt pt pmask1 pSLC_par – itab.selection1 pbase 0 punw1 0 7436 pres2 pdh2 pddef2 punw2 psigma2 pmask2 25. 0.03 3.0 2 - - -

The point mask (pmask1) derived in the initial run is used (i.e. the regression is only calculated for those points previously accepted).

The itab itab.selection1 is used to restrict the regression to the layers or pairs with accepted unwrapped phase.

This regression with unwrapped phases is also more efficient (as the unwrapping is already done). The setting of the quality threshold (maximum phase standard deviation from the regression) and the maximum height correction and linear deformation rate values accepted is also less critical without the necessary unwrapping; permitting to use higher values.

The regression analysis is not explicitly restricted to pairs with baselines $B_{\perp} < 500$, but as only those pairs were previously considered unwrapped phases are only available for pairs within this baseline range.

The results from the regression analysis include:
- height corrections (pdh2),
- linear deformation rate corrections (respectively a first estimate, pddef2),
- point quality measures (phase standard deviation from regression fit, psigma2),
- residual phases (deviation from regression fit, pres2) for each record

These different point data sets and stacks can be displayed using commands as:

pdisdt_pwr24 pt pmask1 19991104.rslc.par pdh2 1 19991104.rmli.par ave.rmli 30.0 1
pdisdt_pwr24 pt pmask1 19991104.rslc.par pddef2 1 19991104.rmli.par ave.rmli 0.01 1
pdisdt_pwr24 pt pmask1 19991104.rslc.par psigma2 1 19991104.rmli.par ave.rmli 1.5 1
prasdt_pwr24 pt pmask1 19991104.rslc.par pres2 - 19991104.rmli.par ave.rmli 12.6 1

The number of “accepted” points with sigma < sigma_max = 3.000 : 12189

The estimated point height corrections, linear deformation rates and phase standard deviations from the regression are shown below:

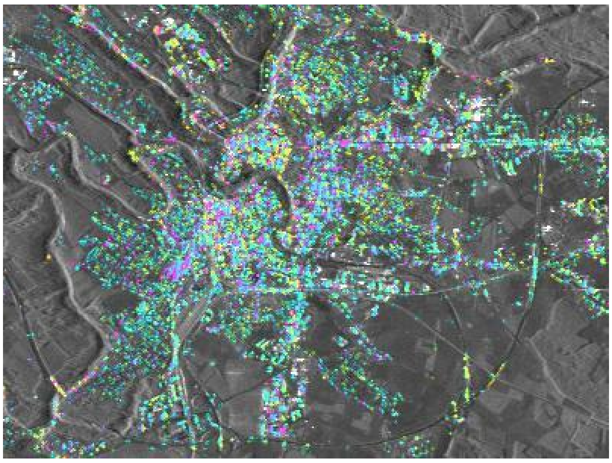
Image of estimated point height corrections (pdh2, color cycle corresponds to 30m).

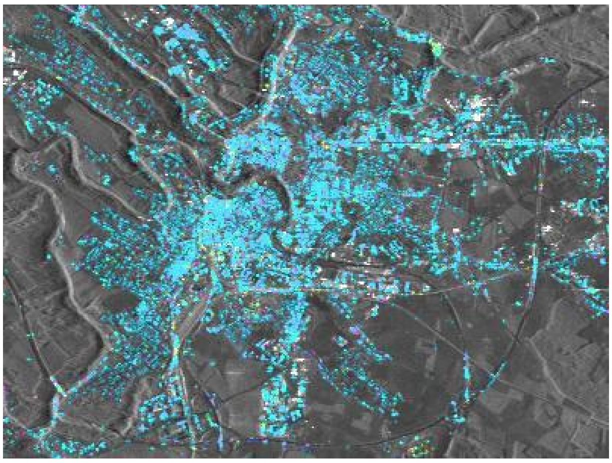
Image of estimated linear deformation rates (pddef2, color cycle corresponds to 0.01m/year).

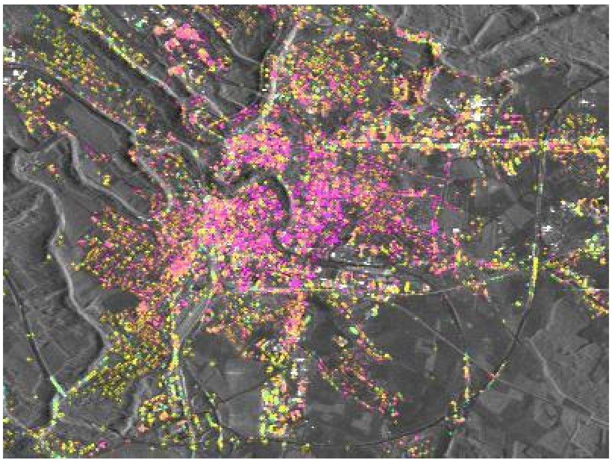
Image of phase standard deviation from regression (psigma2, color cycle corresponds to 1.5 radian). Points closer to the reference point show values around 0.7 radian (red) and points at larger distance values > 1 radian.

The phase standard deviation from the regression increases with increasing distance from values around 0.7 radian closer to the reference point location (< 1 km distance) to values slightly larger than 1 radian for larger distances. This behavior is explained by the phase contributions related to atmospheric path delay heterogeneity and baseline error related phase contributions which both increase with increasing distance.

For the considered pairs, as defined in itab.selection1, all residual phases look spatially "smooth" confirming the correctness of the unwrapping.

4.6. A first solution

The result of this regression corresponds to a "first solution" of the analysis. The point height corrections (pdh2) are used to update the point heights derived from the DEM (pdem), the linear deformation rate estimates (pddef2) are used to update the deformation model (no deformation was assumed), the phase standard deviation psigma2 serves as quality measure, and the residual phases (pres2) contain the deviation from this phase model, which includes non-linear deformation, atmospheric phase, baseline error related phase, and phase noise.

Furthermore, the identified list of "high quality points" defined by pt and pmask2 is an important part of this solution.

The updating of "the model" is done as follows:

```
lin_comb_pt pt pmask2  pdem 1 pdh2 1 phgt1 1 -0. 1. 1. 2 0
cp pddef2 pdef1
```

After this the model is defined by:
- the baselines pbase (initial baselines)
- the point heights phgt1
- the point linear deformation rates pdef1
- the residual phases pres2

This model has its strengths:
- pairs with large baseline errors are excluded
- pairs with strong atmospheric distortions are excluded
- the reliability of the phase unwrapping is high
- the solution is derived using a single reference point
- many (29) observations are considered
- relatively straight forward computation of model
- list of identified high quality points

But the model also has some limitations:
- only orbit based baselines are used
- not all available pairs have been used in the regression
- possibly the spatial coverage might be improved by including further points
- unwrapping errors for individual values of individual points cannot be excluded
- the residual phase has not been interpreted with respect to non-linear deformation, atmospheric distortion, baseline error related phase, and phase noise

The objective of further processing steps is to address these limitations.

5. Inclusion of additional pairs into solution

5.1. Calculating updated differential interferograms

An important advantage of the result from the initial regression analysis (discussed above in Section 4) is the availability of relatively accurate point heights (phgt1) and linear deformation rates (pdef1) for a selection of “high quality” points (pt, pmask2).

Using this point list and model (in particular the improved point heights) the interferometric phase is simulated:

phase_sim_pt pt pmask2 pSLC_par - itab - pbase phgt1 psim_unw0 pdef1 0 0

The updated heights and the estimated linear deformation rates are used. Again, initial and not refined baselines are used. The simulated (unwrapped) phases are subtracted from the complex valued point interferograms to get the point differential interferograms (complex values):

sub_phase_pt pt pmask2 pint - psim_unw0 pdiff0 1 0

Notice that the model which was derived based on only 29 layers is applied to all 56 layers. The resulting 56 differential interferograms can be visualized using:

prasmph_pwr24 pt pmask2 19991104.rslc.par pdiff0 - 19991104.rmli.par ave.rmli 1

and show that even for the pairs with very long baselines the differential interferometric phase looks now relatively smooth. An interpretation (requiring also phase unwrapping) appears feasible.

Examples for a very long baseline and the same long baseline pair as already selected above (pair 32) the differential interferograms are shown below.

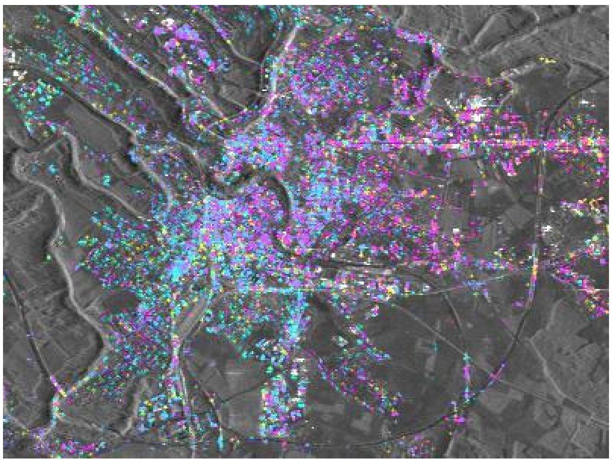

Differential point interferogram (using point heights after initial correction) for very long baseline pair (pair 42, $B_\perp$ -1104m).

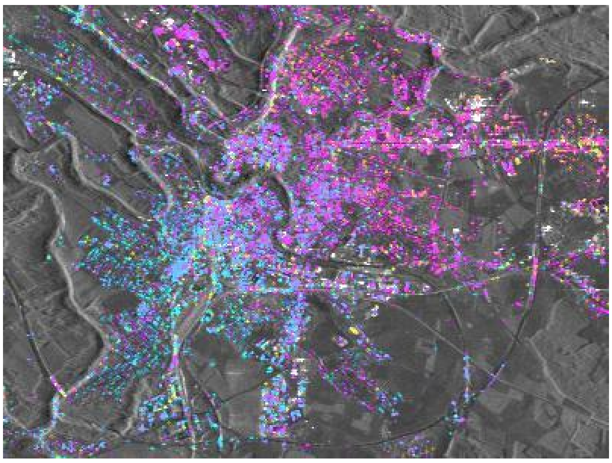

Differential point interferogram (using point heights after initial correction) for long baseline pair (pair 32, $B_\perp$ -567m).

5.2. Regression analysis on updated differential interferograms

On the differential interferogram we run again a regression analysis. The patch wise approach (multi_def_pt) is used, as the differential interferogram is available only in its wrapped (complex valued) form and contains atmospheric phases:

multi_def_pt pt pmask2 pSLC_par - itab pbase 0 pdiff0 1 7436 pres1 pdh1 pddef1 punw1 psigma1 pmask1 3. 0.003 100 1.3 0.9 2 1

The number of “accepted” points with sigma < sigma_max = 1.3: 11974

The height corrections pdh1, the linear deformation rate corrections pddef1 are both relatively small, as the main correction has already been done before. These files as well as the phase standard deviation from the regression fit can be displayed using:

pdisdt_pwr24 pt pmask1 19991104.rslc.par pdh1 1 19991104.rmli.par ave.rmli 10.0 1
pdisdt_pwr24 pt pmask1 19991104.rslc.par pddef1 1 19991104.rmli.par ave.rmli 0.01 1
pdisdt_pwr24 pt pmask1 19991104.rslc.par psigma1 1 19991104.rmli.par ave.rmli 1.5 1

The main interest in this iteration is in seeing if the residual phases look correct for more layers than previously. The residual phases are again displayed using a scaling with two phase cycles per color cycle to make ambiguity phase steps clearly visible:

prasdt_pwr24 pt pmask1 19991104.rslc.par pres1 - 19991104.rmli.par ave.rmli 12.6 1

Each layer is carefully checked for phase steps.

Unwrapping errors (phase steps) were identified for the following layers:
15,17,23,24,41,43,45,48 (i.e. this time only 8 of 56 layers are not correct)

This means a significant improvement from 29 to 48 correctly unwrapped layers.

5.3. Correcting patch related phase unwrapping errors

Now the same procedure could be repeated and possibly a few additional layers could be correctly unwrapped in that manner. The experience shows, that this rather time consuming approach will not necessarily permit to correctly unwrap all layers correctly.

The unwrapping errors seem to be related to:
- remaining orbital fringes (i.e. baseline errors)
- strong atmospheric effects

Both these effects are not really reduced in further iterations, therefore a different approach is more promising.

For some layers with phase steps in pres1 the phase ambiguity errors can be corrected by spatial unwrapping. This is done by first re-wrapping pres1 to get a complex valued data stack with the phases corresponding to those of pres1:

unw_to_cpx_pt pt pmask1 pres1 - pres1.cpx

The complex valued layers are then spatially unwrapped using the minimum cost-flow phase unwrapping approach, using mcf_pt:

mcf_pt pt pmask1 pres1.cpx - - - pres1.cpx.unw 20 4 7436 0

The resulting unwrapped real-valued phase images are again displayed and carefully checked for phase steps using:

prasdt_pwr24 pt pmask1 19991104.rslc.par pres1.cpx.unw - 19991104.rmli.par ave.rmli 12.6 1

In this relatively simple case (small area, low deformation rates, urban area) the spatial unwrapping is successful for all the remaining 8 layers. An example of a pres1 layer with phase steps and the same layer without obvious unwrapping errors after the re-wrapping and spatial unwrapping (pres1.cpx.unw) is shown below:

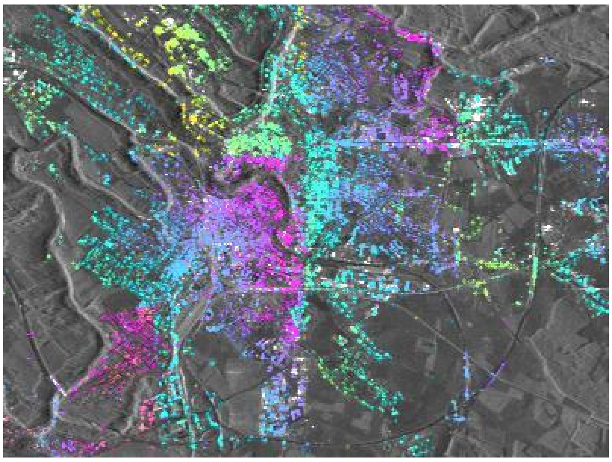

Residual phase (pres1) point image which clearly indicates phase unwrapping errors (pair 23, $B_\perp$ 364m).

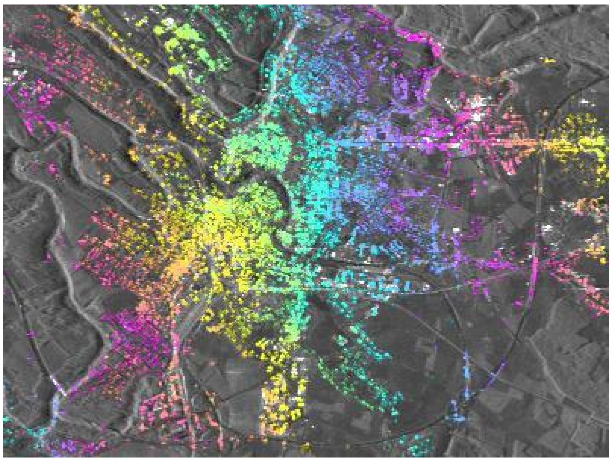

Residual phase (pres1.cpx.unw) with corrected unwrapping (pair 23, $B_\perp$ 364m).

It cannot be expected that the presented procedure will always solve the “unwrapping problem” as elegantly as in this relatively simple case. In other examples it may be experiment a while trying to include some more “challenging layers”.

Here some general recommendations:

(1) Typically, it is easier to unwrap the residual phase than to unwrap the corresponding differential interferogram. The unwrapped phase of the differential interferogram can subsequently be calculated from the unwrapped residual phases, and the other parameters obtained in the regression analysis.
(2) Keep the already correctly unwrapped layers and try to increase this list (do not restart from the beginning). The above spatial unwrapping is an example for this strategy, as the already unwrapped phases may be kept.
(3) Accept that there may be image areas and/or observations (= layers) which cannot easily be integrated. These are typically areas with a “poor spatial sampling”. Such “poor spatial sampling” can be related to a very low point density or to high deformation rates (especially if the deformation is temporally non-uniform). Causes for entire layers being of too low quality, include snow cover (or other very significant change to the scene) as well as more sensor/processing related factors such as very

different Doppler parameters or poor co-registration. Such layers may be explicitly excluded from the analysis as they may contribute more problems and signal noise than actual information.

And more specific recommendations to solve the unwrapping problem:

(4) One possibility to modify the spatial unwrapping is to apply a spatial filtering (using spf_pt) to the re-wrapped residual phases prior to the spatial unwrapping (using mcf_pt). To get the unwrapped phases of the unfiltered re-wrapped residual phases the program unw_model_pt can be used (with the unwrapped filtered re-wrapped residual phases as model).
(5) mcf_pt supports the use of masks and weights (e.g. difficult areas which cause errors but which are not of interest can be masked or the use of weights to improve the unwrapping can be tried).
(6) Unwrapping in the temporal dimension (e.g. after refinement of the baselines for the already "solved" layers and/or after subtraction of initial atmospheric phase layers (estimated by strong spatial filtering of the residual phase layers) is an other possibility.

5.4. Calculating unwrapped differential interferogram phase from residual phase

From the accepted residual phases (here pres1.cpx.unw) the unwrapped phases of the differential interferogram can be calculated. The relation used is as follows:

pdiff0_unw(i) = regression model(i) + pres(i) - pres(iref) + ref_point_phase(i)
with

pdiff0_unw(i):	the unwrapped phase of the differential interferogram pdiff0
regression model(i):	the regression model phase (calculated from pdh1,pddef1)
pres(i):	the accepted residual phase (here pres1.cpx.unw) of layer i
pres(iref):	the accepted residual phase of the reference layer
ref_point_phase(i):	the pdiff0 phase of the reference point (here nr. 7436) of layer i

This calculation is done as follows:

Calculation of regression model phase:
phase_sim_pt pt pmask1 pSLC_par - itab - pbase pdh1 psim_unw2 pddef1 2 0
(notice that option 2 is used which is specifically included to calculate the regression plane phase values based on the height correction (pdh1), the linear deformation rate correction (pddef1), the perpendicular baseline component, and the time difference)

Calculation of reference point phase:
The reference point phase of the differential interferogram is the phase of the selected reference point. The differential interferogram stack pdiff0 is complex valued, so the reference point phase is not directly accessible (in float format). The unwrapped phase file (generated above in using multi_def_pt), punw1, contains the real valued phase of the differential interferogram pdiff0. Values should be between minus PI and plus PI. This can be checked using:

prt_pt pt pmask1 punw1 7436 1 2 - 1 56

In spite of unwrapping problems in the regression analysis the real valued phase at the reference point will be correct.

The different real valued components are then combined using lin_comb_pt:

```
/bin/rm ptmp1 ptmp2
lin_comb_pt pt pmask1 psim_unw2 – punw1 - ptmp1 - 0.0 1.0 1.0 2 1 7436
lin_comb_pt pt pmask1 ptmp1 - pres1.cpx.unw -  ptmp2 - 0.0 1.0 1.0 2 1
lin_comb_pt pt pmask1 ptmp2 - pres1.cpx.unw 47 pdiff0_unw - 0.0 1.0 -1.0 2 1
```

5.5. Consistency checking of unwrapping

pdiff0_unw can be compared with the unwrapped phase stack punw1 which was generated by multi_def_pt using the program pdis2dt:

```
pdis2dt pt pmask1 19991104.rslc.par punw1 20 pdiff0_unw 20 19991104.rmli.par 12.6 0
pdis2dt pt pmask1 19991104.rslc.par punw1 23 pdiff0_unw 23 19991104.rmli.par 12.6 0
```

The first comparison is for layer 20 which appeared correctly unwrapped (when considering pres1). Only very few points differ by a 2π ambiguity.

The second comparison is for a layer 23 which showed a phase unwrapping problem in pres1. As expected the unwrapped phases differ significantly with pdiff0_unw showing the corrected solution. For whole sections the phases differs by a 2π ambiguity.

For a more quantitative evaluation of the difference between the two unwrapping solutions the difference between the two solutions is calculated and thres_msk_pt is used to “count” the identical and not identical values (make a copy of pmask1 first to avoid that it is overwritten with the modified mask values):

```
/bin/rm ptmp
lin_comb_pt pt pmask1 punw1 - pdiff0_unw - ptmp - 0.0 1.0 -1.0 2 1
prasdt_pwr24 pt pmask1 19991104.rslc.par ptmp - 19991104.rmli.par ave.rmli 12.6 1

/bin/cp pmask1 pmask1_tmp
thres_msk_pt pt pmask1_tmp ptmp 23 -0.1 0.1

1: 11974 -> 11828
2: 11974 -> 11746
3: 11974 -> 11545
17: 11974 -> 11098
23: 11974 ->  5309
```

This comparison shows that individual phases of individual points may differ at this stage of the analysis (which results in a slight uncertainty on the exact model point heights and deformation rates as well as on the deviation from the model, which is related to the atmospheric phase and the phase noise).

At this stage the phases shall mainly be used to refine the baseline model. The available quality is fully satisfactory for this purpose. It has to be kept in mind though, that the phase unwrapping done is not yet perfect for each point and layer.

5.6. Combining correctly unwrapped layers into one stack

In this example we could just use pdiff0_unw as the unwrapped phase. In other cases some layers may not be correct in pdiff0_unw (which was calculated to get a solution for some layers which were incorrect in the solution by multi_def_pt), so to show how the good layers of the two stacks are combined, we use the solution from the spatial unwrapping (i.e. pdiff0_unw) only for those layers which were previously incorrect. This is done using lin_comb_pt:

```
/bin/cp punw1 punw1a
lin_comb_pt pt pmask1 pdiff0_unw 15 pdiff0_unw 15 punw1a 15 0.0 1.0 0.0 2 1
lin_comb_pt pt pmask1 pdiff0_unw 17 pdiff0_unw 17 punw1a 17 0.0 1.0 0.0 2 1
lin_comb_pt pt pmask1 pdiff0_unw 23 pdiff0_unw 23 punw1a 23 0.0 1.0 0.0 2 1
lin_comb_pt pt pmask1 pdiff0_unw 24 pdiff0_unw 24 punw1a 24 0.0 1.0 0.0 2 1
lin_comb_pt pt pmask1 pdiff0_unw 41 pdiff0_unw 41 punw1a 41 0.0 1.0 0.0 2 1
lin_comb_pt pt pmask1 pdiff0_unw 43 pdiff0_unw 43 punw1a 43 0.0 1.0 0.0 2 1
lin_comb_pt pt pmask1 pdiff0_unw 45 pdiff0_unw 45 punw1a 45 0.0 1.0 0.0 2 1
lin_comb_pt pt pmask1 pdiff0_unw 48 pdiff0_unw 48 punw1a 48 0.0 1.0 0.0 2 1
```

As a result we get the unwrapped phase stack punw1a with correct unwrapping for the "large majority of points", as required for baseline refinement.

Based on the unwrapped phase of the differential interferogram we calculate the unwrapped phases of the initial interferograms, pint, by adding back what was previously subtracted:

```
phase_sim_pt pt pmask1 pSLC_par - itab - pbase phgt1 psim_unw0 pdef1 0 0
sub_phase_pt pt pmask1 punw1a - psim_unw0 pint_unw 0 1
```

6. Baselines refinement

6.1. Calculation of refined baselines

A baseline error causes a phase error which depends more or less linearly on the distance between a pair of points. As we want to work in the end with a single reference point this means very substantial phase errors, up to several phase cycles. Therefore, we refined the baseline model based on the interferogram data itself. This is done by optimizing the baselines such that the deviations between modeled and calculated phases are minimal in a least squares sense. The result is not the physically correct baseline, as other large-scale phase trends (e.g. in the atmospheric path delay) get partly compensated by the refinement of the baseline. On the other hand the remaining orbital fringes which are observed in the case of a baseline error could be compensated by assuming an atmospheric phase correction with a relatively strong range dependence. In general, the atmospheric phase is not expected to show significant linear trends (especially if very large areas are considered).

We strongly recommend to refine the baselines.

The refinement of the baselines is done for each layer (not just those with obvious orbit fringes in the differential interferogram).

Known heights and unwrapped phases are used for the refinement. The question if the original heights available (e.g. in the Luxemburg example the heights derived based on the SRTM 3”

DEM) or the improved ones (the actual point heights derived in the regression analysis) should be used. Using the improved heights will reduce the standard deviation in the least squares optimization of the baseline refinement and statistical quality measures will indicate a higher quality of the refinement. In spite of this ***we strongly recommend to use the original heights***, as this means that the original heights are used as reference and not modified ones which may include an offset or linear trend.

Another question is if atmospheric phases shall be subtracted prior to the baseline refinement. Subtracting atmospheric phases will strongly reduce the standard deviation in the least squares optimization of the baseline refinement and statistical quality measures will indicate a higher quality of the refinement. Nevertheless, only very minimal modification of the baseline can be expected as all larger scale phase trends, including residual orbital phase trends from using incorrect baseline models, are removed as “atmospheric phase”. Consequently, ***we strongly recommend not to apply any atmospheric phase correction prior to the baseline refinement.***

The last question which needs to be considered is what to do about areas with significant deformation. Deformation phases influence the baseline refinement. Two strategies appear reasonably. The first one is to avoid areas with significant deformation. This is done by just using the stable areas for the baseline refinement – something which can be done in all those cases where large parts of the scatterers are almost stable. The second strategy would be to first compensate the deformation phase (based on the already estimated deformation rates) and then to use these compensated phases for the baseline refinement.

In the Luxemburg example the first strategy is used. Based on the already estimated deformation rate, pdef1, we select all points with very low deformation rates between –2mm/year and +2mm/year. For this purpose we copy the mask for the accepted high quality points to a new name:

/bin/cp pmask1 pdef1_mask

and apply thres_msk_pt to select among those accepted points the ones with very low deformation rates:

thres_msk_pt pt pdef1_mask pdef1 1 -0.002 0.002

11724 points out of 11974 points meet this criteria.

Prior to the baseline refinement we make a backup of the baseline stack:

/bin/cp pbase pbase.orbit

The baseline refinement is done:

- for all 56 layers
- based on the original (SRTM based) heights pdem
- considering only the almost stable points

base_ls_pt pt pdef1_mask pSLC_par - itab - pint_unw pdem pbase 0 1 1 1 1 1. > base_ls_pt.out

The standard output is piped into the ASCII file base_ls_pt.out (as quality information and for documentation purposes).

To see if the refinement was successful the quality information needs to be checked. A low RMS altitude error is a good indication for a successful refinement. Notice that the RMS altitude error depends on the phase error and the perpendicular baseline. For short baselines a high RMS altitude error does not necessarily mean a problem in the optimization, as it can still correspond to a small phase RMS error. Have a look at the baselines and RMS altitude errors for the Luxemburg example. The refinement is judged successful for all layers.

```
grep "b_perp (t=center) (m):" base_ls_pt.out
grep "RMS altitude error (m):" base_ls_pt.out
/bin/cp pbase pbase.051026
```

After the refinement it is recommended to make another backup of the baseline stack.

6.2. Application of refined baselines

In a next step the refined baselines are applied. In order to avoid having to go through the phase unwrapping again the unwrapped phases are used (knowing that a few of the values may actually still be on the wrong ambiguity).

As a first step the point heights and linear deformation rates are updated for pdh1 and pddef1 as determined in last use of multi_def_pt:

```
/bin/cp phgt1 phgt0
/bin/cp pdef1 pdef0
/bin/cp pmask1 pmask0
lin_comb_pt pt pmask1  phgt0 1 pdh1 1 phgt1 1 -0. 1. 1. 2 0
lin_comb_pt pt pmask1  pdef0 1 pddef1 1 pdef1 1 -0. 1. 1. 2 0
```

The updated heights and linear deformation rates are then used to simulate the interferometric phases using the refined baselines:

```
phase_sim_pt pt pmask1 pSLC_par - itab - pbase phgt1 psim_unw0 pdef1 0 1
```

The simulated phases, psim_unw0, are subtracted from the real-valued unwrapped interferogram pint_unw:

```
sub_phase_pt pt pmask1 pint_unw - psim_unw0 pdiff0_unw 0 0
```

And def_mod_pt is used to conduct a regression analysis (using a single reference point):

```
def_mod_pt pt pmask0 pSLC_par - itab pbase 1 pdiff0_unw 0 7436 pres1 pdh1 pddef1 punw1
psigma1 pmask1 25. 0.03 2.0 2 - - -
```

A high threshold (here 2.0 radian) is used as the phases still include the atmospheric distortions. The number of points for which the standard deviation from the regression sigma is below the indicated sigma_max=2.000 is 11937.

The height corrections, deformation rate corrections, phase standard deviations, and residual phases are displayed using:

pdisdt_pwr24 pt pmask1 19991104.rslc.par pdh1 1 19991104.rmli.par ave.rmli 10.0 3
pdisdt_pwr24 pt pmask1 19991104.rslc.par pddef1 1 19991104.rmli.par ave.rmli 0.002 3
pdisdt_pwr24 pt pmask1 19991104.rslc.par psigma1 1 19991104.rmli.par ave.rmli 1.5 3
prasdt_pwr24 pt pmask1 19991104.rslc.par pres1 - 19991104.rmli.par ave.rmli 12.6 1

We note the following:

- Significant corrections to the height and linear deformation rates are found. These corrections are somewhat "patchy" which is expected as the previous model used was derived with multi_def_pt using patches.
- The overall flatness of the residual phases confirms that the baseline refinement was successful.
- A few layers show strong atmospheric signals: 17,37,38,45

The model is updated for these corrections using:

/bin/cp phgt1 phgt0
/bin/cp pdef1 pdef0
/bin/cp pmask1 pmask0
lin_comb_pt pt pmask1 phgt0 1 pdh1 1 phgt1 1 -0. 1. 1. 2 0
lin_comb_pt pt pmask1 pdef0 1 pddef1 1 pdef1 1 -0. 1. 1. 2 0

6.3. Discussion of the solution obtained after the baseline refinement

It is expected that further iterations using the unwrapped phases will not result in significant corrections. Checking this can be done using the sequence:

phase_sim_pt pt pmask1 pSLC_par - itab - pbase phgt1 psim_unw1 pdef1 0 1
sub_phase_pt pt pmask1 pint_unw - psim_unw1 pdiff0_unw1 0 0

def_mod_pt pt pmask0 pSLC_par - itab pbase 1 pdiff0_unw1 0 7436 pres1 pdh1 pddef1 punw1 psigma1 pmask1 25. 0.03 2.0 2 pdh_err1 pdef_err1 ppc_err1

using phase_sim_pt, sub_phase_pt, and def_mod_pt) confirms this expectation: corrections are very small and not patchy.

Another test that is suggested here is to re-run the regression but excluding the layers with the strongest atmospheric distortions – this to check their effect on the model and phase standard deviation. This is done using the following sequence:

/bin/cp itab itab.selection3
nedit itab.selection3 & (and set flags for layers 17,37,38,45 to 0)

phase_sim_pt pt pmask1 pSLC_par - itab.selection3 - pbase phgt1 psim_unw3 pdef1 0 1
sub_phase_pt pt pmask1 pint_unw - psim_unw3 pdiff0_unw3 0 0

def_mod_pt pt pmask0 pSLC_par - itab.selection3 pbase 1 pdiff0_unw3 0 7436 pres3 pdh3 pddef3 punw3 psigma3 pmask3 25. 0.03 2.0 2 pdh_err3 pdef_err3 ppc_err3

pdisdt_pwr24 pt pmask1 19991104.rslc.par pdh3 1 19991104.rmli.par ave.rmli 1.0 1
pdisdt_pwr24 pt pmask1 19991104.rslc.par pddef3 1 19991104.rmli.par ave.rmli 0.0005 1

pdisdt_pwr24 pt pmask1 19991104.rslc.par psigma3 1 19991104.rmli.par ave.rmli 1.5 1

And to compare these results with the results for the complete set:

pdis2dt pt pmask1 19991104.rslc.par pdh1 1 pdh3 1 19991104.rmli.par 1.0 1
pdis2dt pt pmask1 19991104.rslc.par pddef1 1 pddef3 1 19991104.rmli.par 0.0005 1
pdis2dt pt pmask1 19991104.rslc.par psigma1 1 psigma3 1 19991104.rmli.par 1.5 1
pdis2dt pt pmask1 19991104.rslc.par pres1 1 pres3 1 19991104.rmli.par 6.3 1
pdis2dt pt pmask1 19991104.rslc.par pdh_err1 1 pdh_err3 1 19991104.rmli.par 1. 1
pdis2dt pt pmask1 19991104.rslc.par pdef_err1 1 pdef_err3 1 19991104.rmli.par 0.001 1

Observations:
- The corrections found (pdh3, pddef3) are small, but significant and correspond in their shape somewhat to the atmospheric distortions.
- Furthermore, the phase standard deviation (psigma3) is significantly reduced.
- The residual phases are very similar in appearance, but there are phase differences of up to about 0.2 radian
- The reduction in the phase standard deviation results in a reduction of the estimation uncertainty for the regression model, i.e. pdh_err and pdef_err are reduced as well.

These observations lead to some questions such as:
- Which model is the correct one?
- Should the 4 layers with stronger atmosphere be used at all? if yes how?

For the moment we don't go into a detailed investigation of these questions, but continue the processing using all layers. Some confirmation to do this comes from the fact that the size of the corrections found when ignoring the layers with the strongest atmospheric distortions remained for most points within the related estimation uncertainties (i.e. ABS(pdh3) < pdh_err1, ABS(pddef3) < pdef_err1).

The model available at this stage is already quite advanced in that:
- unwrapped phases are available for all layers
- refined baselines were determined
- point heights and linear deformation rates (and related estimation uncertainties) were estimated based on the entire stack of observations

The two main remaining limitations of this result are the following:
- there are some unwrapping errors (for some points of some layers)
- the residual phases have not been interpreted with respect to non-linear deformation, atmospheric phase, and phase noise

7. Interpretation of residual phases with respect to atmospheric phase, non-linear deformation phase and phase noise and unwrapping improvement

7.1. Introduction

The residual phases were obtained by subtracting the bi-linear regression model (linear with respect to the perpendicular baseline components and linear with respect to acquisition time differences). This was done for phase differences relative to a selected reference point (location). The residual phases are available as real-valued (i.e. unwrapped) phases. Residual phases outside the interval (-π,π) are possible.

The residual phases can be considered as a sum of the following 3 components:
- non-linear deformation phase
- atmospheric phase
- phase noise

The non-linear deformation phase corresponds to the total deformation phase minus a linear deformation trend. Non-uniform movements occur for many different reasons and can have very different characteristics, on the temporal scale "everything" between uniform movements and movements at a single moment in time (e.g. during an earthquake) occur, including accelerated movements and movement with a periodic component. The sampling of the displacement achieved with the interferometric observations may not in every case be good enough to reliably retrieve the displacement history. This particularly under the consideration that the phases are originally only available in wrapped form. On the spatial scale deformation can be at very large scale (e.g. tectonic displacements) to deformation of the individual point (e.g. sinking of a specific house). The level of non-linear deformation phase can be very significant (e.g. in the case of an accelerating landslide). In the case of a high non-linear deformation component it is likely that the actual phase level cannot be correctly retrieved due to unwrapping problems. The unwrapping tends to move the values close to those corresponding to the long term linear trend. What is noted in such a case is that the values will show a larger phase noise for the observations of the non-linear behavior.

Atmospheric path delay effects are caused by heterogeneity in the tropospheric water vapor content and (typically to a lesser degree) in the ionosphere. Resulting phase errors are predominantly at larger spatial scale. Nevertheless, atmospheric errors are at all scales so that removing the larger scale effects cannot be expected to completely remove the atmospheric distortions. On a temporal scale the atmospheric phase distortions are largely uncorrelated. The level of the atmospheric phase distortions is most of the time below one phase cycle but with some exceptions.

Phase noise is temporally and spatially uncorrelated. The level of the phase noise is directly related to the "quality" of a point.

The separation of the 3 components of the residual phases is not a simple task and there is not a general "best solution" to it. It is strongly recommended to spend a moment on the related strategic planning. As described above some compromises are needed, this because the temporal and spatial characteristics of the different components overlap. An example of such strategic planning is presented in the following for the Luxemburg example.

7.2. Strategic planning for the interpretation of the residual phases

In the following we conduct a strategic planning for the for the interpretation of the residual phases for the Luxemburg example. The planning presented and the resulting strategy are specific for this example. Other examples may have different characteristics and require different strategies.

Observations and interpretations:
- The differential interferograms (and residual phases) appear relatively smooth in that phase differences between neighboring points are much smaller than π in most cases.

- Some differential interferograms show phase signals of the order of π which are most likely related to atmospheric distortions. These atmospheric distortions appear temporally uncorrelated (different locations of bubbles in different pairs, bubbles present in pair 47 – 17 are not observed in pairs 47 – 16 and 47 – 18. Apart from the most obvious atmospheric distortions at lower level are expected and observed.
- No significant (e.g. rates > 3mm/year) larger scale (e.g. > 50 pixels) deformation signals are obvious (i.e. phase signals of the mentioned dimension with a consistent temporal characteristics (e.g. all pairs before 1994 consistently show the deformation).
- A few small scale deformation signals are observed, i.e. the linear deformation rate shows similar significant values (e.g. > 1mm/year or < -1mm/year) for local groups of points.
- For some individual points the linear deformation rate differs significantly (e.g. by more than 1 mm/year) from that of its neighboring points. The corresponding observation in the differential interferogram (without subtraction of deformation phase) is that there are points with a clearly different phase as compared to their neighbors (and this difference is temporally systematic, i.e. similar differences are observed for similar time intervals).

Strategic decisions:

- Based on these observations we decide that the detection of large scale non-linear deformation is not in the focus of our interest – this means that we can assign all large scale deviations from the linear regression model to the atmosphere. This decision has the consequence that we will not detect any large scale non-linear deformation.
- The main interest will be on the local deformation signals – i.e. small localized groups of points showing a similar behavior. Non-linear components in this local deformation is of interest. An important aspect will be to ensure the highest possible quality in the phase unwrapping.
- Furthermore, we are interested in the deformation of individual points. Here an important aspect will be to get a clear image of the reliability of the observation.
- The interpretation and phase unwrapping benefit from a reduction of phase noise. In the IPTA stacks phase differences between a reference point an a second point are considered. The noise of such a difference depends on the noise at the reference point and the noise at the second point. Selection of a point with a very high quality is one way to reduce the noise of the phase differences. Another possibility is to apply spatial filtering at the reference point (an option of spf_pt supports this operation) and to use this “artificial reference” with a very low phase noise.

Practical consequences and resulting processing steps:

1) Estimation of atmospheric phases: Estimate large scale components of residual phases (using spatial filtering) and call these atmospheric phases. No temporal evaluation of these large scale phases is necessary, no large scale non-linear phase trends are part of the model. Subtract atmospheric phases from differential interferograms. To achieve residual large scale phases below about 1 radian an iterative estimation scheme needs to be applied. The atmospheric phases are estimated from the residual phases.
2) Reduce phase noise by using the spatially filtered signal as reference.
3) Redo estimation of linear deformation rates and phase unwrapping: for the identified points the point heights, the atmospheric phases, and the refined baselines are used to recalculate linear deformation rates and to redo the phase unwrapping.
4) Visualization of deformation histories with related auxiliary information (including quality information)

5) Manual and automated checking of result (in particular unwrapping) and in particular the unwrapping (e.g. through a comparison with spatially unwrapped residual phases); remove uncertainties

7.3. Estimation of atmospheric phases:

The atmospheric phases are estimated from the residual phases pres1 by spatial filtering using the program spf_pt. To get some experience with the influence of the filter size and weighting function type indicated we run the filter for different filter window sizes (indicated on the command line is the filter radius in range pixels, the number of azimuth pixels is adjusted such that a corresponding distance is covered). For a filer window radius of 25 pixels and weights that linearly decrease with increasing distance the command is:

spf_pt pt pmask1 19991104.rslc.par pres1 pres1_spf_25_1 - 2 25 1 –

Similarly, the filtering is repeated using a 50 pixel radius and a 10 pixel radius. For layer 17, which is one with strong atmospheric artifacts, the filtered residual phases and the difference between the residual phase and the filtered residual phase (i.e. what remains apart from the atmospheric phase) look as shown below.

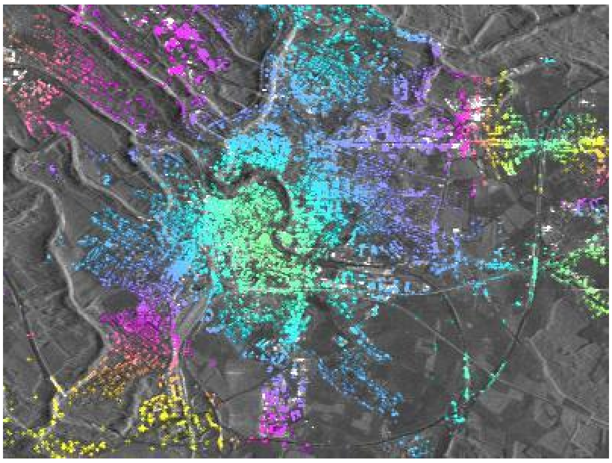

Pair 17: residual phase spatially filtered using a filter window radius of 50 pixels (display with 2π per color cycle).

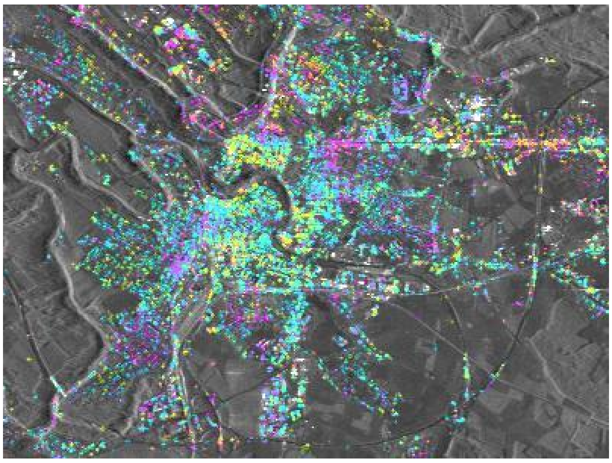

Pair 17: difference between residual phase and spatially filtered residual phase using a filter window radius of 50 pixels (display with π per color cycle).

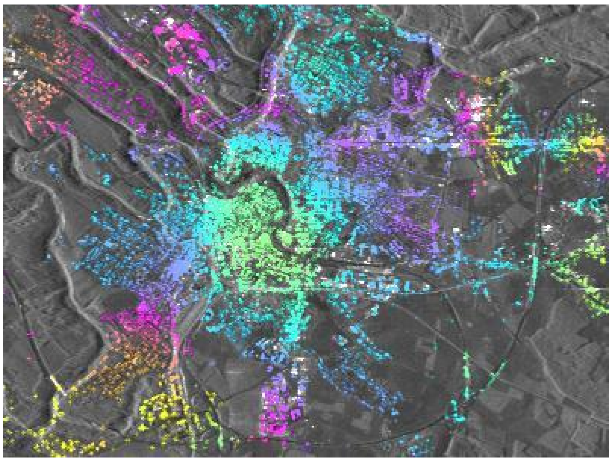

Pair 17: residual phase spatially filtered using

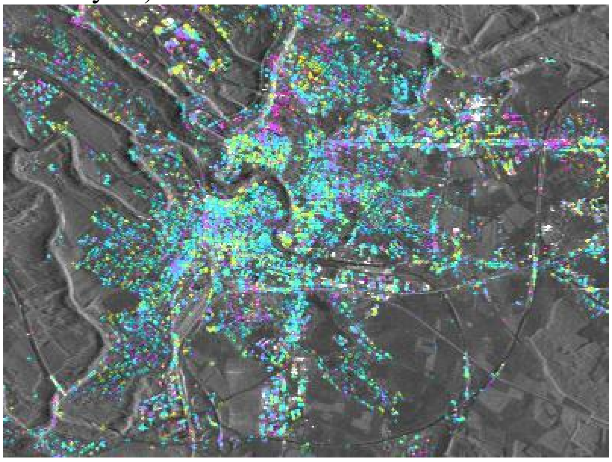

Pair 17: difference between residual phase and

a filter window radius of 25 pixels (display with 2π per color cycle).

spatially filtered residual phase using a filter window radius of 25 pixels (display with π per color cycle).

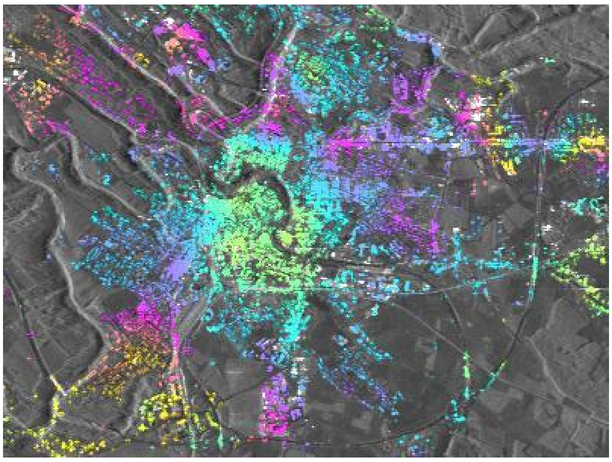

Pair 17: residual phase spatially filtered using a filter window radius of 10 pixels (display with 2π per color cycle).

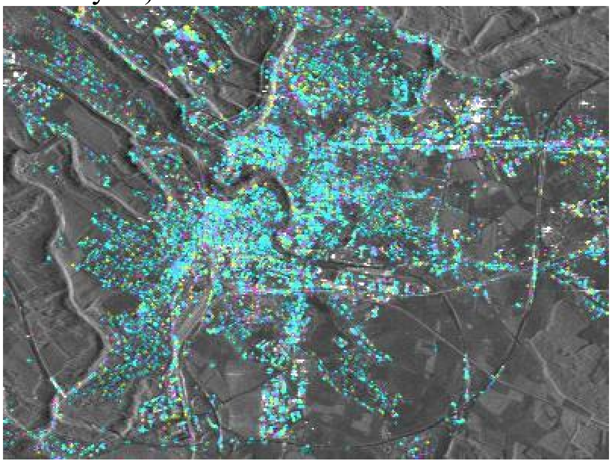

Pair 17: difference between residual phase and spatially filtered residual phase using a filter window radius of 10 pixels (display with π per color cycle).

For pair 17 the larger filter windows (radii 50 and 25) remove most of the larger scale residual phase , but there remain smaller areas with phase which appears to be related to the atmospheric effect and not to non-linear deformation. Based on this our preferred choice is to use the filtering with the smallest filter. Doing this, we have to keep in mind that we tend to remove all non-linear deformation at scales larger than about 10 range pixels (or 200m on the ground). For the Luxemburg example this choice may be acceptable as the identified deformations are all very localized - but such choice cannot be recommended in general, more often a radius of 25 pixels may be the smallest reasonable choice.

The filtered residual phase is renamed to “atmospheric phase”

/bin/cp pres1_spf_10_1 patm1

Now, this stack corresponds to the atmospheric distortions at the individual acquisition dates, including the date of the reference scene (in the auto-interferogram layer). To calculate the combined atmospheric distortion which affects an interferogram pair the atmosphere for the reference layer has to be subtracted from the atmosphere which correspond to the second acquisition. We calculate the atmospheric corrections for the interferometric pairs using:

lin_comb_pt pt pmask1 patm1 - patm1   47 patm1x - 0. 1. -1. 2 1

These atmospheric phases can then be subtracted from the differential interferogram:

sub_phase_pt pt pmask1 pdiff0_unw - patm1x pdiff1_unw 0 0

7.4. Reduce phase noise by using the spatially filtered signal as reference.

To achieve a reduction of the phase noise of the interferometric phases relative to the reference point we filter replace the reference point phases with spatially filtered phases. This is adequate if the area around the reference location can be assumed stable. This is done using the related mode of spf_pt:

spf_pt pt pmask1 19991104.rslc.par pdiff1_unw pdiff1_unwa - 2 25 0 - 7436 0

A filter window with a radius of 25 pixels was used for the filtering.

7.5. Redo estimation of linear deformation rates and phase unwrapping

As a next step we run a regression analysis on the differential interferograms. The subtraction of the atmospheric phases and the use of the filtered reference phase may result in slight corrections to the point heights and linear deformation rate estimates and the phase standard deviation psigma is expected to be reduced:

def_mod_pt pt pmask0 pSLC_par - itab pbase 1 pdiff1_unwa 0 7436 pres2 pdh2 pddef2 punw2 psigma2a pmask2 25. 0.03 2.0 2 pdh_err2a pdef_err2a ppc_err2a

For comparison reasons we also run def_mod_pt for pdiff0_unw (without atmospheric corrections, unfiltered reference) and for pdiff1_unw (with atmospheric corrections, unfiltered reference). The resulting phase standard deviations are shown below.

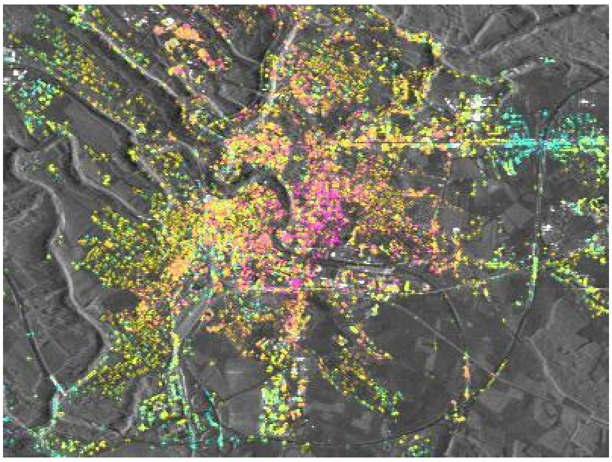

Phase standard deviation from regression fit without subtraction of atmospheric corrections and without reference point filtering.

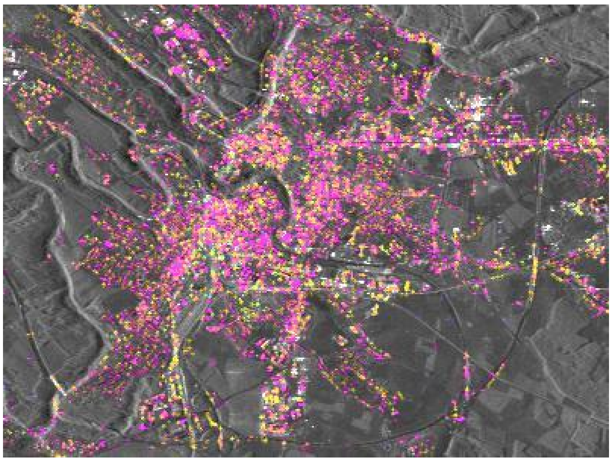

Phase standard deviation from regression fit with subtraction of atmospheric corrections and without reference point filtering.

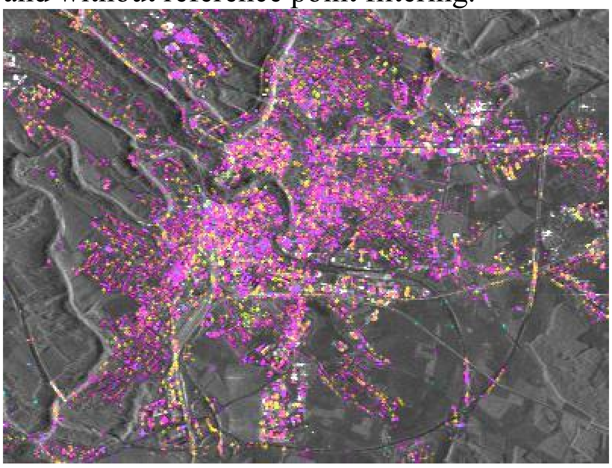

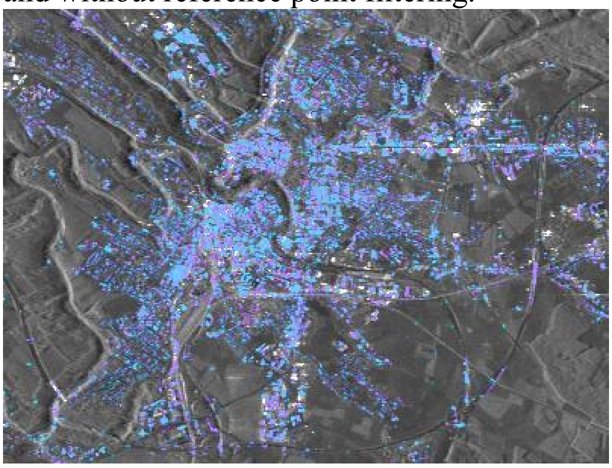

Phase standard deviation from regression fit with subtraction of atmospheric corrections and with reference point filtering.

Estimated uncertainty of linear deformation rate estimate with subtraction of atmospheric corrections and with reference point filtering.

The subtraction of the atmospheric corrections had the effect that the phase standard deviation became more or less independent of the location, respectively the distance from the reference point. The use of a spatially filtered phase as reference only slightly reduced the phase noise, which is a confirmation that the selected reference point was of high quality. Together with the phase standard deviation the estimation uncertainties for the point height correction and linear deformation rate become independent of the location. The values of the statistically estimated deformation rate uncertainty show is now of the order of 0.1 mm/year. The value of this error estimate after subtracting the atmospheric phases is somewhat questionable and should not be taken uncritically as the accuracy measure for the deformation rates.

7.6. Visualization of deformation histories with related auxiliary information

As a next step we visualize the deformation histories. For this purposes we need to calculate a stack which contains the series of deformation phases and the related phase noise which is defined as:

displacement phase = phase of linear displacement + non-linear deformation phase + noise

For this we update the point heights and linear deformation rates for the last corrections found:

```
lin_comb_pt pt pmask1  phgt1 1 pdh2 1 phgt2 1 -0. 1. 1. 2 0
lin_comb_pt pt pmask1  pdef1 1 pddef2 1 pdef2 1 -0. 1. 1. 2 0
```

We calculate the deformation phase (ptmp1) corresponding to the estimated linear deformation rates:

```
/bin/rm ptmp1
phase_sim_pt pt pmask1 pSLC_par - itab - pbase - ptmp1 pdef2 1 0
```

And we add the last residual phase which contains the non-linear deformation phase as well as the phase noise.

```
lin_comb_pt  pt pmask1 ptmp1 - pres2 - pdef_phase1 - 0.0 1. 1. 2 1
```

The atmospheric phase is not included here. The combined phase is then converted to line-of-sight displacement values (negative displacement values correspond to subsidence):

```
dispmap_pt pt pmask1 pSLC_par itab pdef_phase1 phgt2 pdisp1 0
```

A SUN Rasterfile of the displacement at the earliest date (layer 1) is then generated (to be used as optical reference to select points):

```
prasdt_pwr24 pt pmask1 19991104.rslc.par pdisp1   1 19991104.rmli.par ave.rmli 0.05 0
```

```
vu_disp pt pmask1 pSLC_par itab pdisp1 pdef2 phgt2 psigma2a pdh_err2a pdef_err2a - pdisp1.ras
```

For the large majority of the points the deformation rate estimated is below 2mm/year with the individual observations deviating by less than 0.45cm (corresponding to 1 radian) from the curve with no significant change to the point quality over time (i.e. similar statistical deviations at all times). These points / observations / estimates have a high reliability. The time history of the deformation contains little additional information as compared to the linear deformation rate.

7.7. Discussion of deformation histories

In the following the findings for some specific points are discussed in more detail. Most of these points are selected as they illustrate typical “problems” which can occur with the processing and interpretation.

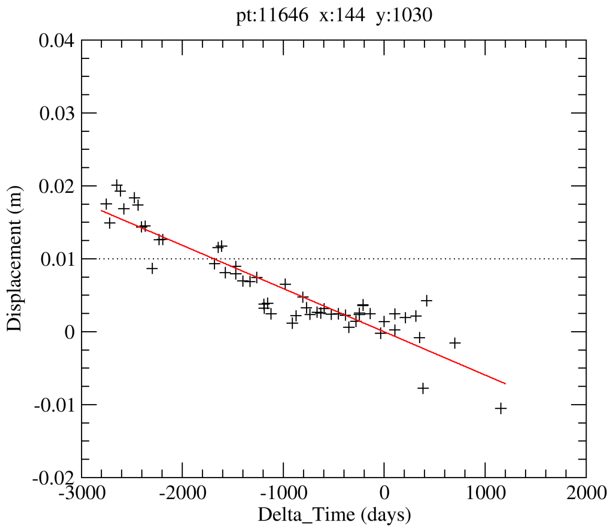

Displacement history point 11646: Between 1992 and 2004 a line-of-sight displacement of about 3 cm (away from the sensor) is observed. All values lie within 0.7cm (corresponding to $\pi/2$) of the linear curve with a phase standard deviation significantly below 1 radian. The uniform deformation model appears to adequately represent the measurements. No distinct outliers or unwrapping errors are apparent.

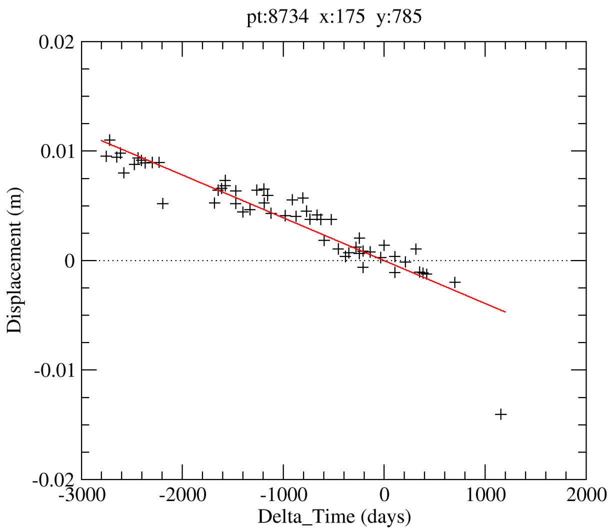

Displacement history point 8734: Between 1992 and 2004 a line-of-sight displacement of about 1.5 cm (away from the sensor) is observed. All values except the last one lie within 0.35cm (corresponding to $\pi/4$) of the linear curve with a phase standard deviation significantly below 0.5 radian. The uniform deformation model appears to adequately represent the measurements (except the last one).The last value appears to be an outlier. Possible interpretations include a degradation of the point quality and a (speculative) acceleration of the deformation. Setting the last point on a 2π higher ambiguity would result in a similar (but positive outlier).

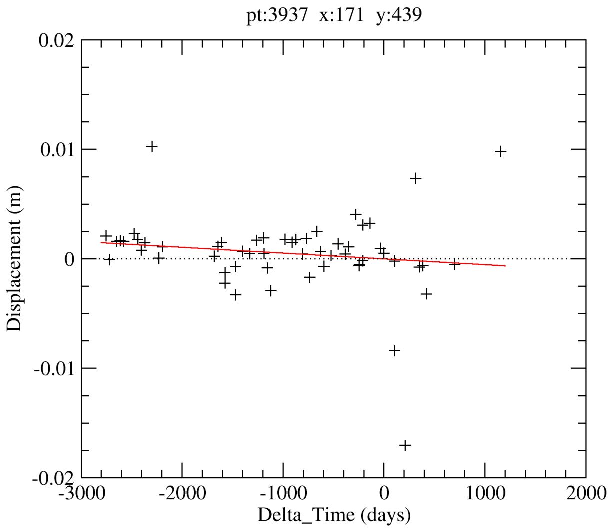

Displacement history point 8734: In this case the observations are closely grouped around an almost flat curve for the time period between day –3000 and day 0 (with one exception). After day 0 the deviation from the regression curve is much more significant with positive and negative deviations larger than 0.7 cm (corresponding to π/2) for 4 of the 8 observations. It is not obvious how different phase unwrapping might better align these observations. The most likely explanation is that the point quality became bad after day 0.

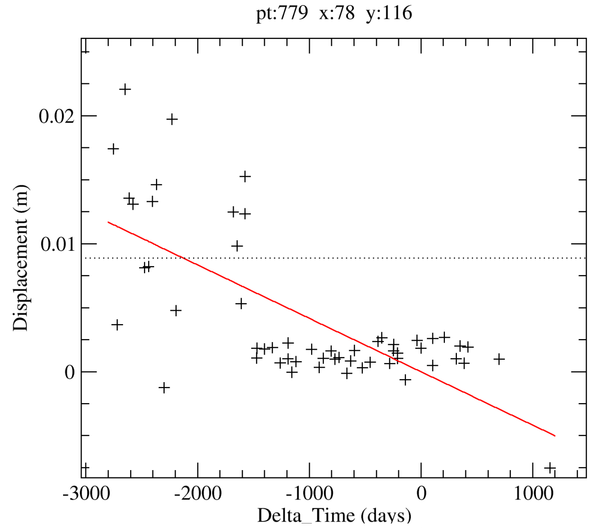

Displacement history point 779: This case resembles the previous one quite closely except that the poor point quality is observed at the beginning of the time series and not at its end. A possible explanation could be that this point was only initiated around day –1500 (the scatterer could be a new house, for example). What is significantly different from the previous example is that the linear deformation rate estimated deviates strongly from stability, this in spite of the high quality observations clearly indicating stability for the time period after day –1500 (with only the last observation deviating more significantly).

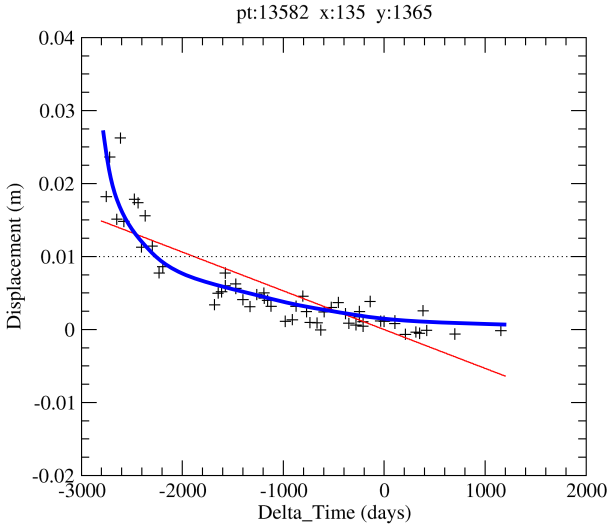

Displacement history point 13582: This deformation history is particularly interesting, as it shows a clearly non-linear behavior. In the beginning (1992-1993) the deformation rate is higher (with about 2 cm in two years) than after 1994 (with less than 1 cm in 10 years). The small deviations of the observations from the non-linear deformation curve drawn in blue is a confirmation of the correctness of the phase unwrapping.

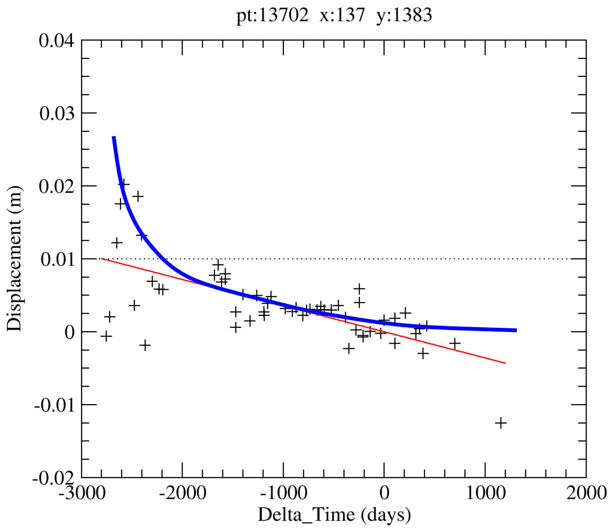

Displacement history point 13702: This deformation history resembles somewhat to that of point 779. Nevertheless, considering that it is located very closely to point 13582 (and other points indicating similar behavior as point 13582) we can also speculate that it indicates a similar deformation history as point 13582, but with a phase unwrapping error for many of the early observations (and maybe the very last one). The exact same non-linear deformation curve that matches the observations of point 13582 was drawn again in blue and it seems that it matches the point 13702 observations, particularly if we "correct the unwrapping" by adding 2.8cm to four of the early observations.

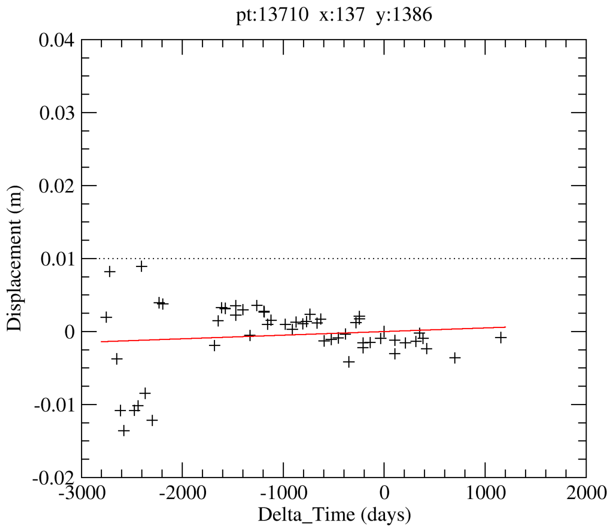

Displacement history point 13710: Another point near the previous two and again we can speculate that a different phase unwrapping will lead to a similar non-linear deformation history. Notice that the linear deformation rate estimate indicates a very slight uplift in this case. Again the overall phase standard deviation is quite low so that this point is not necessarily rejected. What can be observed is that the linear rate is not consistent with its (spatial) neighbors, and the deviation from the linear fit is significantly higher for the early observations.

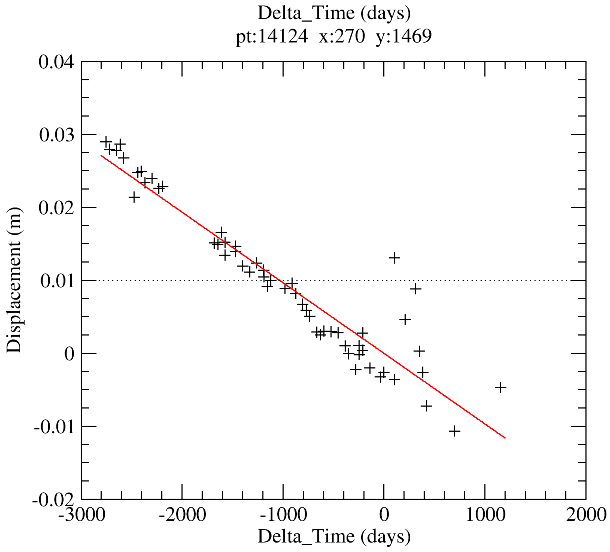

Displacement history point 14124: This deformation history shows a relatively fast deformation. Until about day 0 the values are all very close to the regression line. After that the values deviate more significantly. A possible interpretation is that the deformation even accelerated slightly after day 0 and that some of the values after that day are on the wrong ambiguity (unwrapping errors). Shifting the late points by 2.8cm down results in a nice looking (and therefore plausible) non-linear deformation history.

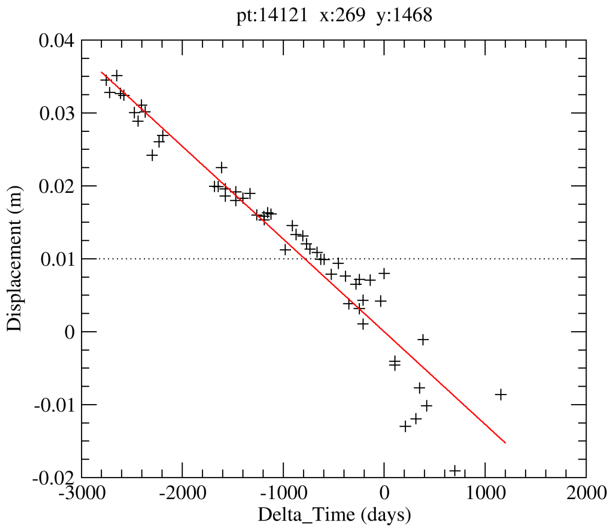

Displacement history point 14121: The point 14121 deformation history supports the interpretation of an accelerated deformation at the closely located point 14124. For the exception of the very last point such acceleration is indeed observed here. (The very last point, which is not as well connected to the series temporally, may be shifted down by 2.8 cm to also match the accelerated deformation curve.

7.8. Manual and automated checking of result and in particular the unwrapping

At this stage we check the temporal and spatial consistency of the phase unwrapping.

Considering on one hand deformation histories, as the ones shown above, and on the other hand checking the spatial consistency of the residual phases by comparing the residual phases to the phases obtained after rewrapping and spatially unwrapping, we note the following:

- There are some points for which a different unwrapping of a few values may result in values which match a relatively smooth non-linear deformation curve significantly better
- For some values spatial unwrapping would result in a different value

In the Luxemburg example points with “larger” deformation rates (> 3mm/year) are found for relatively small areas, and often these points are rather aligned than covering a 2D area. Consequently, spatial and temporal unwrapping cannot necessarily be expected to match.

To improve the unwrapping in this case without too much reducing the number of points accepted and maybe even more important, without rejecting to many of those more interesting points with significant deformation is not trivial.

The quality of the unwrapping can be improved by better unwrapping and by rejecting unreliable values or points. In the following we describe a possible approach.

We restart from original complex differential interferogram generated using:

- refined baselines (pbase)
- estimated atmosphere (patm1, patm1x)
- point height estimates (phgt2)
- pmask1
- using reference point filtering

phase_sim_pt pt pmask1 pSLC_par - itab - pbase phgt2 psim_unw0 - 0 1
sub_phase_pt pt pmask1 pint - psim_unw0 pdiff0 1 0
sub_phase_pt pt pmask1 pdiff0 - patm1x pdiff1 1 0
spf_pt pt pmask1 19991104.rslc.par pdiff1 pdiff1a - 0 25 0 - 7436 1

On this complex valued differential interferogram we apply a slight temporal filtering. The filter length is selected long enough, that the filter includes several observations (to get a reduction of the phase noise) but short enough, so that the phase value variation shall be smaller than π (filtering of the complex values does not make sense if these values differ very strongly). Notice that this filtering is done prior to the unwrapping. Notice also, that option 1 for reference point phase offset removal has been selected to bring all the differential interferograms to a level around zero phase (otherwise this phase offset between layers will influence subsequent temporal filtering).

For the temporal filtering a long time interval, but with a maximum number of 7 values to be considered is indicated. Weights linearly decreasing with time distance are used. The filtering is rerun 3 times, to strongly reduce the noise but without using a too long interval (resp. too many neighboring observastions):

```
tpf_pt pt pmask1 pSLC_par itab pdiff1a   pdiff1a.1 0 1000 1 7
tpf_pt pt pmask1 pSLC_par itab pdiff1a.1 pdiff1a.2 0 1000 1 7
tpf_pt pt pmask1 pSLC_par itab pdiff1a.2 pdiff1a.tpf 0 1000 1 7
```

Based on the filtered differential interferograms a regression analysis is conduced:

```
def_mod_pt pt pmask1 pSLC_par - itab pbase 1 pdiff1a.tpf 1 7436 pres2 pdh2 pddef2 punw2
psigma2 pmask2 5. 0.03 2.0 2 pdh_err2 pdef_err2 ppc_err2
```

and resulting time series are visualized:

```
/bin/rm ptmp1
phase_sim_pt pt pmask1 pSLC_par - itab - pbase - ptmp1 pddef2 1 0
lin_comb_pt  pt pmask1 ptmp1 - pres2 - pdef_phase1 - 0.00001 1. 1. 2 0
dispmap_pt pt pmask1 pSLC_par itab pdef_phase1 phgt2 pdisp1 0
prasdt_pwr24 pt pmask1 19991104.rslc.par pdisp1   1 19991104.rmli.par ave.rmli 0.05 0
vu_disp pt pmask1 pSLC_par itab pdisp1 pddef2 phgt2 psigma2 pdh_err2 pdef_err2 -
pdisp1.ras
```

These smoothed temporal curves shall be used as references for the unwrapping of the unfiltered values, but only in those cases where the filtered curves appear correct. The standard deviation of the temporally filtered values from the linear regression, psigma2, can be used for this purpose. A strong deviation from the linear behavior is an indication for either a very non-uniform deformation history, or for unwrapping errors which resulted in this stronger deviation.

Using a threshold on psigma2 is used to reject points with high standard deviations:

```
/bin/cp pmask1 pmask1_thresh
thres_msk_pt pt pmask1_thresh psigma2 1 0.0 0.60
```

Instead of 11938 only 11614 points are accepted.

For the accepted points (pmask1_thresh) the unwrapped phases of pdiff1a.tpf, punw2, are used as models to unwrap pdiff1a, the unfiltered differential interferograms:

```
unw_model_pt pt pmask1_thresh pdiff1a - punw2 pdiff1a.unw 7436
```

A regression analysis is then run on the unfiltered unwrapped differential interferograms:

def_mod_pt pt pmask1_thresh pSLC_par - itab pbase 1 pdiff1a.unw 0 7436 pres2 pdh2 pddef2 punw2 psigma2 pmask2 5. 0.03 2.0 2 pdh_err2 pdef_err2 ppc_err2

No the phase standard deviation from the linear regression is a combination of the non-linearity of the deformation and the noise. We would like to discard noisy values only but keep non-linear deformation histories. For this we first estimate the non-linear estimation – this is again done by a similar temporal filtering as used beforehand, but this time applied to the unwrapped phases (the residual phases) – and then we a coherence in the temporal dimension on the deviations of the measurements from the non-linear deformation estimates (here called pres2.noise):

tpf_pt pt pmask1_thresh pSLC_par itab pres2   pres2.1 2 1000 1 7
tpf_pt pt pmask1_thresh pSLC_par itab pres2.1 pres2.2 2 1000 1 7
tpf_pt pt pmask1_thresh pSLC_par itab pres2.2 pres2.tpf 2 1000 1 7
lin_comb_pt pt pmask2 pres2 - pres2.tpf - pres2.noise - 0.0 1. -1. 2 0
cct_pt pt pmask1_thresh 19991104.rslc.par pres2.noise pcct 2 8

Residual phases, temporal filtered residual phases and deviations (noise) can be displayed using:

dis_data pt pmask1 pSLC_par itab 3 pres2 pres2.tpf pres2.noise 0 pdisp1.ras -3. 3.

The temporal coherence is displayed using:

pdisdt_pwr24 pt pmask1_thresh 19991104.rslc.par pcct   1 19991104.rmli.par ave.rmli 1.0 1

And values with high temporal coherence (= low noise) are selected using:

/bin/cp pmask1_thresh pmask1_thresh2
thres_msk_pt pt pmask1_thresh2 pcct 1 0.7 1.0

Resulting in 11112 accepted points.

This result can again be visualized using vu_disp:

/bin/rm ptmp1
phase_sim_pt pt pmask1_thresh2 pSLC_par - itab - pbase - ptmp1 pddef2 1 0
lin_comb_pt pt pmask1_thresh2 ptmp1 - pres2 - pdef_phase1 - 0.00001 1. 1. 2 0
dispmap_pt pt pmask1_thresh2 pSLC_par itab pdef_phase1 phgt2 pdisp1 0
prasdt_pwr24 pt pmask1_thresh2 19991104.rslc.par pdisp1 1 19991104.rmli.par ave.rmli 0.05 0
vu_disp pt pmask1_thresh2 pSLC_par itab pdisp1 pddef2 phgt2 psigma2 pdh_err2 pdef_err2 - pdisp1.ras

7.9. Identification of points of temporary low quality

As observed above (see discussion on deformation time series examples) it happens that a certain point is of good quality for only a part of the total time period covered by the observations. In particular, it happens that inadequate quality is observed at the beginning of the time series – corresponding to a point that only started to become a persistent point-like scatterer at a given date – and at the end of the time series – corresponding to a point that is only a persistent point-like scatterer until a given date. Construction of new infrastructure and modification of infrastructure can explain such behavior.

Notice that points with a low quality for most of the observations will be discarded due to the relative (statistical) weight of the low quality observation. Therefore, no points with only a few high quality observations, e.g. at the end of the time period are identified in the above processing. With the particular temporal coverage of the Luxemburg stack with 12 observations in 1992-1993 followed by a gap in 1994 and only very few observations between 2001 and 2003 low quality is observed mainly for these two periods. While the 12 observations for 1992-1993 observations permit a relatively reliable estimation of thepoint quality during 1992-1993, this is not as reliably possible for 2001-2003.

In the following it is shown how the point quality is determined for 1992-1993 and how points with too low quality during this period can be discarded.

To selectively work with the first 12 observations the itab itab.start is generated (a copy of itab with 0 flags for layers 13 to 56):

cp itab itab.start
e itab.start & (set flags for layers 13 to 56 to zero).

Then a regression analysis is run on this reduced stack, using the unwrapped differential interferometric phases:

def_mod_pt pt pmask1_thresh2 pSLC_par - itab.start pbase 1 pdiff1a.unw 0 7436 pres2.start pdh2.start pddef2.start punw2.start psigma2.start pmask2.start 5. 0.01 2.0 2

The standard deviations from the linear regression found for this interval is then used to characterize the point quality during this period. Values with too high phase standard deviation are discarded using:

/bin/cp pmask1_thresh2 pmask1_thresh2start
thres_msk_pt pt pmask1_thresh2start psigma2.start 1 0.0 1.1

Resulting in a reduced selection of 10402 accepted points. The result (with the specific phase standard deviation is displayed using:

prasdt_pwr24 pt pmask1_ thresh2start 19991104.rslc.par pdisp1 1 19991104.rmli.par ave.rmli 0.05 0
vu_disp pt pmask1_thresh2start pSLC_par itab pdisp1 pddef2 phgt2 psigma2.start pdh_err2 pdef_err2 - pdisp1.ras

The main result of this analysis on the first 12 acquisitions is the mask pmask1_thresh2start.

7.10. Consolidation of the result

For the accepted points we calculate the unwrapped phase, pint_unw2, of the initial interferogram. This is done by using the unwrapped differential interferogram phase pdiff1a.unw (after the reference point filtering) as model to unwrap the differential interferogram pdiff1. To this phase the simulated phase and the atmospheric phases which were previously subtracted are added back:

```
/bin/rm ptmp1
unw_model_pt pt pmask2 pdiff1 - pdiff1a.unw pdiff1.unw 7436
phase_sim_pt pt pmask2 pSLC_par - itab - pbase phgt2 psim_unw0 - 0 1
sub_phase_pt pt pmask2 pdiff1.unw - patm1x ptmp1 0 1
sub_phase_pt pt pmask2 ptmp1 - psim_unw0 pint_unw2 0 1
```

Using these unwrapped phases we determine a last update / consolidation of the model for the accepted points:

```
/bin/rm ptmp1 ptmp2
phase_sim_pt pt pmask2 pSLC_par - itab - pbase phgt2 psim_unw0 - 0 1
sub_phase_pt pt pmask2 pdiff1a.unw - patm1x ptmp1 0 1
sub_phase_pt pt pmask2 ptmp1 - psim_unw0 ptmp2 0 1
unw_model_pt pt pmask2 pint - ptmp2 pint_unw2 7436
```

```
def_mod_pt pt pmask1_thresh2start pSLC_par - itab pbase 1 pdiff1a.unw 0 7436 pres2 pdh2 pddef2 punw2 psigma2 pmask2 5. 0.03 2.0 2
```

The model elements are then updated, including the point heights:

```
lin_comb_pt pt pmask2 phgt2 1 pdh2 1 phgt3 1 -0. 1. 1. 2 0
```

the linear deformation rates:

```
/bin/cp pddef2 pdef3
```

and the atmospheres (in pres2 a few layers show locations with spatially correlated phases):

```
spf_pt pt pmask2 19991104.rslc.par pres2 pres2_spf_10_1 - 2 10 1 -
lin_comb_pt pt pmask2 patm1 - pres2_spf_10_1 - patm2 1 -0. 1. 1. 2 0
lin_comb_pt pt pmask2 patm2 - patm2 47 patm2x 1 -0. 1. -1. 2 0
```

For the updated model we calculate again the differential interferograms (starting from the unwrapped phases):

```
phase_sim_pt pt pmask2 pSLC_par - itab - pbase phgt3 psim_unw2 pdef3 0 1
sub_phase_pt pt pmask2 pint_unw2 - psim_unw2 pdiff2.unw 0 0
sub_phase_pt pt pmask2 pdiff2.unw - patm2x pdiff3.unw 0 0
```

Here we apply a removal of the reference point phase offset to get residual phases around zero phase (without phase offset):

```
spf_pt pt pmask2 19991104.rslc.par pdiff3.unw pdiff3a.unw - 2 250 0 - 7436 1
```

On this we apply another regression analysis to estimate parameters as the phase standard deviation and the height and linear deformation rate estimation error estimates:

def_mod_pt pt pmask2 pSLC_par - itab pbase 1 pdiff3a.unw 0 7436 pres3 pdh3 pddef3 punw3 psigma3 pmask3 5. 0.01 1.2 2 pdh_err3 pdef_err3

Using a maximum phase standard deviation of 1.2 radian results in 10401 accepted points. To use a very low threshold value here is not desired, as this will discard all the points with non-linear deformation (as we didn't subtract this part from the differential interferogram).

The point height and linear deformation rate correction obtained in this last step are very small (further iteration without change of the unwrapping does not lead to a modification of the result).

This result is then again used to update the model:

```
/bin/rm ptmp1
lin_comb_pt pt pmask3 phgt3 1 pdh3 1 phgt4 1 -0. 1. 1. 2 0
lin_comb_pt pt pmask3 pdef3 1 pddef3 1 pdef4 1 -0. 1. 1. 2 0
```

and the result is visualized:

```
phase_sim_pt pt pmask3 pSLC_par - itab - pbase - ptmp1 pdef4 1 0
lin_comb_pt  pt pmask3 ptmp1 - pres3 - pdef_phase1 - 0.00001 1. 1. 2 0
dispmap_pt pt pmask3 pSLC_par itab pdef_phase1 phgt4 pdisp1 0
prasdt_pwr24 pt pmask3 19991104.rslc.par pdisp1   1 19991104.rmli.par ave.rmli 0.05 0
vu_disp pt pmask3 pSLC_par itab pdisp1 pdef4 phgt4 psigma3 pdh_err3 pdef_err3 - pdisp1.ras
```

7.11. Estimation and visualization of non-linear deformation

What was displayed above by vu_disp is the deformation observations including the phase noise and non-linear deformation. One way to explicitly determine the non-linear deformations is to apply temporal filtering on these results:

```
tpf_pt pt pmask3 pSLC_par itab pres3   pres3.1 2 1000 1 7
tpf_pt pt pmask3 pSLC_par itab pres3.1 pres3.2 2 1000 1 7
tpf_pt pt pmask3 pSLC_par itab pres3.2 pres3.tpf 2 1000 1 7
```

To display the "non-linear deformation model" with the unfiltered deformation history we use:

```
phase_sim_pt pt pmask3 pSLC_par - itab - pbase - ptmp1 pdef4 1 0
lin_comb_pt  pt pmask3 ptmp1 - pres3.tpf - pdef_phase2 - 0.00001 1. 1. 2 0
dispmap_pt pt pmask3 pSLC_par itab pdef_phase2 phgt4 pdisp2 0
dis_data pt pmask3 pSLC_par itab 2 pdisp1 pdisp2 0 pdisp1.ras -0.02 0.02
```

Examples for 4 points are shown below:

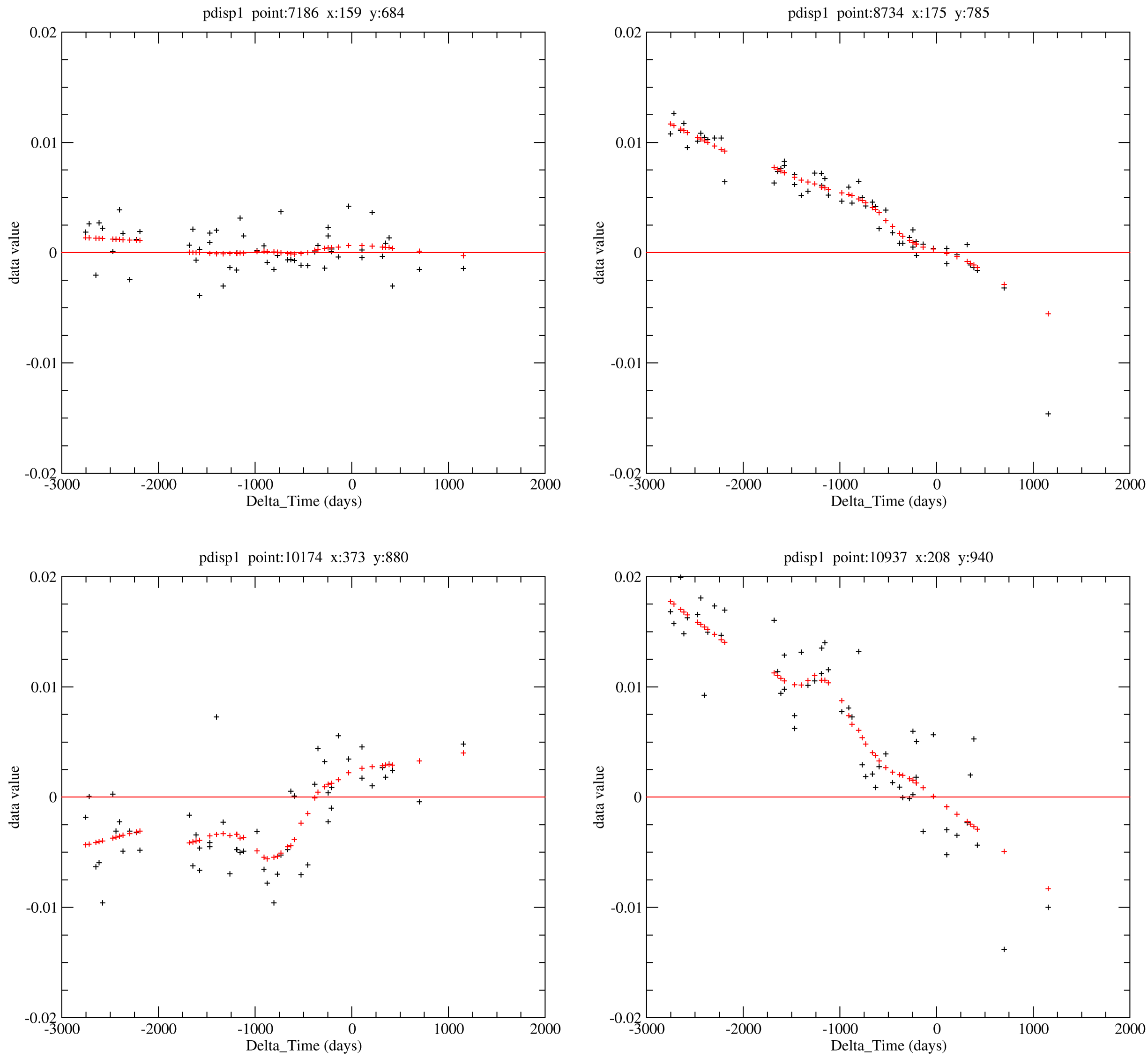

Examples of non-linear deformation histories (red) and corresponding unfiltered observations (containing non-linear deformation and phase noise).

8. Expansion of result to more points

8.1. Objectives

In the IPTA processing it is possible to build upon an existing solution and check additional points if a solution can be found for them. There are two major advantages of this possibility:

1) The possibility to later-on add points make the decision to reject points much easier.
2) For the additional points an already accepted point is used as local reference in the integration step. Using a local reference has advantages such as lower atmospheric and non-linear deformation phases.

The expansion of an existing result to further points is done using the following main steps:

1) Expand the existing solution (i.e. the point heights, the linear deformation rate, the atmospheric phases, if existing the non-linear deformation) to further points by interpolation.

2) Calculate the differential interferogram for the combined point list (points with solution and additional points)
3) Locally conduct regression analyses on the differential interferogram phases using the accepted points as local reference to determine point height corrections, linear deformation rate corrections, and a quality measure for the new points.
4) Update point list and solution to include additional accepted points.

8.2. Expand the existing solution

The program expand_data_pt supports the expansion of an existing solution to additional points by interpolation. The point with an existing solution are defined by a point list and point mask (here pt and pmask3). For these points the data file or data stack (e.g. patm2) contains values. These values are interpolated (or extrapolated) to additional points defined in a second point list and point mask. In the specific example shown here the second point list is identical with the first one but the second point mask is not indicated, that is all points of the point list are tested without consideration of a point mask. So all previously rejected points are tested again – but this time the regression analysis will be conducted relative to a local accepted reference.

The expansion is done for the atmospheric phases:

```
expand_data_pt pt pmask3 19991104.rslc.par patm2 pt - patm2_ex - 2 512 1 256
prasdt_pwr24 pt - 19991104.rslc.par patm2_ex - 19991104.rmli.par ave.rmli 6.3 1
lin_comb_pt pt - patm2_ex - patm2_ex 47 patm2x_ex - 0.0 1.0 -1.0 2 1
```

and the linear deformation rate:

```
expand_data_pt pt pmask3 19991104.rslc.par pdef4 pt - pdef4_ex - 2 512 1 256
prasdt_pwr24 pt - 19991104.rslc.par pdef4_ex - 19991104.rmli.par ave.rmli 0.03 1
```

For the terrain heights a different approach is used. The idea here is to use accepted point height corrections but to use the initial terrain heights from the DEM for the additional points to be checked. This combination is achieved using:

```
lin_comb_pt pt - phgt4 1 pdem 1 ptmp1 1 0.0 0.0 1.0 2 0
lin_comb_pt pt - phgt4 1 pdem 1 ptmp2 1 0.0 1.0 1.0 2 1
lin_comb_pt pt - ptmp2 1 ptmp1 1 phgt4_ex 1 0.0 1.0 -1.0 2 1
```

The result is checked using:

```
pdis2dt pt - 19991104.rslc.par phgt4 1 phgt4_ex 1 19991104.rmli.par 256. 2
```

8.3. Calculate the differential interferogram for the combined point list

Then the differential interferograms are calculated for the combined point list (pt without mask):

```
phase_sim_pt pt - pSLC_par - itab - pbase phgt4_ex psim_unw0 pdef4_ex 0 1
sub_phase_pt pt - pint - psim_unw0 pdiff0_ex 1 0
sub_phase_pt pt - pdiff0_ex - patm2x_ex pdiff1_ex 1 0
```

8.4. Regression analyses using the accepted points as local reference

For these differential interferograms regression analyses are conducted for the additional points using nearby accepted points as local references:

expand_pt pt pmask3 pt pmask3_ex pSLC_par itab pbase 1 pdiff1_ex pdiff1_ex 1 pres1_ex pdh1_ex pddef1_ex psigma1_ex 1.0 15. 0.01 2 -1 -1 25

As a result additional points of adequate quality are found. And for these additional points point height corrections and linear deformation rates are determined (as correction to the previous estimates obtained by interpolation).

These corrections can be displayed using:

pdisdt_pwr24 pt pmask3_ex 19991104.rslc.par pdh1_ex 1 19991104.rmli.par ave.rmli 30.0 2
pdisdt_pwr24 pt pmask3_ex 19991104.rslc.par pddef1_ex 1 19991104.rmli.par ave.rmli 0.01 2
pdisdt_pwr24 pt pmask3_ex 19991104.rslc.par psigma1_ex 1 19991104.rmli.par ave.rmli 1.5 0

8.5. Update point list and solution to include additional accepted points.

The model is then updated for the new point list which includes the additional “good points” found:

lin_comb_pt pt pmask3_ex phgt4_ex 1 pdh1_ex 1 phgt1_ex 1 -0. 1. 1. 2 1
lin_comb_pt pt pmask3_ex pdef4_ex 1 pddef1_ex 1 pdef1_ex 1 -0. 1. 1. 2 1

the updated deformation rate is displayed using:

pdisdt_pwr24 pt pmask3_ex 19991104.rslc.par pdef1_ex 1 19991104.rmli.par ave.rmli .005 1

Some of the additional points found are indicating relevant deformation rates (e.g. around pixel 135, 273) as shown in the Figures below:

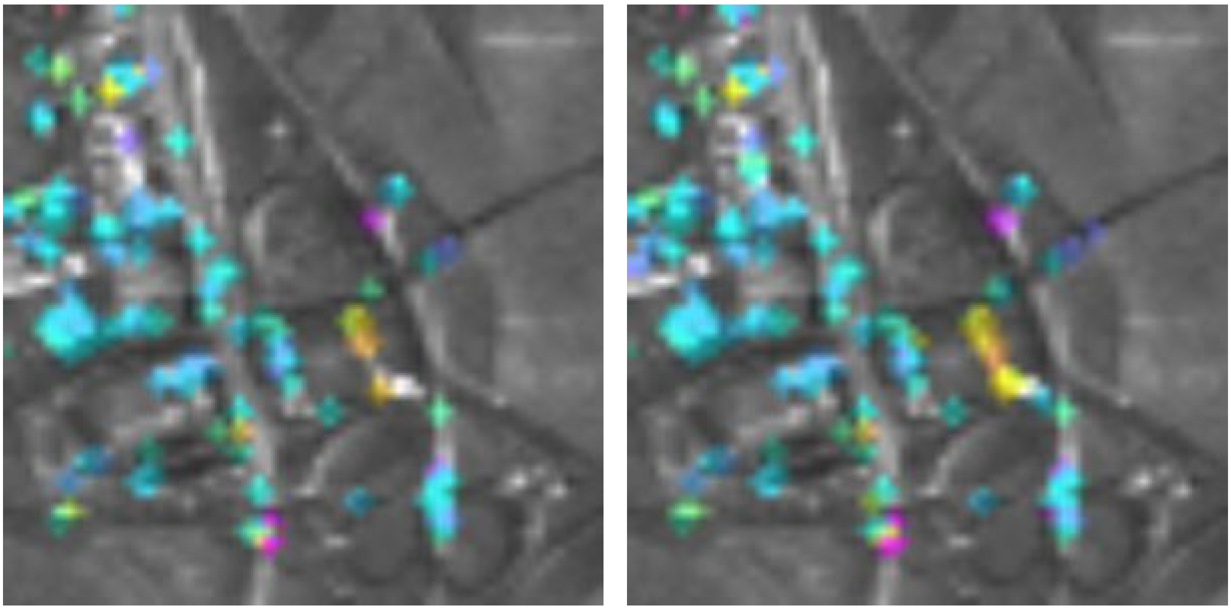

In this subsection of the Luxemburg area the expansion resulted in additional points confirming the observed deformation near the image center (yellow color).

8.6. Quality checking

It is clear that these additional results need to be checked similar to the checking done for the initially accepted points. This checking is not presented here, therefore the example will be continued with the previous result (without expansion). The expansion is understood as a separate section just included to show how more points can be included.

8.7. Checking all points

It is worth mentioning, that the above approach to include additional points can be applied even to all points (possibly for larger test areas it is necessary to do this patch-wise) to avoid very big data sets.

9. Transformation of solution into map geometry

9.1. Point data geocoding concept

As is common in SAR image analysis some of the processing or investigation is done in the SAR slant range / Doppler coordinates. Then at a later stage geocoding – i.e. transformation from the range-Doppler to map geometry is done; an essential step for the comparison and integration with "other" information and for visualization purposes.

To some degree this approach also applies to an IPTA analysis. So far the processing was primarily done in the SAR coordinates – and now we would like to transform the results in the selected map geometry.

But there are also significant differences from the "normal" approach because of the investigation being done on point lists and not on 2D raster data sets. In SAR geometry the data are organized in vector data format. Based on the point location (SAR image coordinates, that is column and row numbers) we are also able to generate 2D displays. Now, instead of a resampling of raster data we just need to calculate for each point its coordinates in the map geometry. Then 2D displays in map geometry can be generated similarly to 2D displays in SAR geometry from the identical point data sets and point data stacks.

9.2. Calculating point coordinates

The point coordinates are calculated using the previously determined refinement polynomial (determined in the refinement used in the geocoding of the average intensity image and transformation of the DEM heights from map to SAR geometry) contained in the DIFF parameter file 19991104.diff_par. is done using:

pt2geo pt pmask3 pSLC_par - itab phgt4 Luxemburg.utm.dem_par 19991104.diff_par 1 5 pt_map pmap pmapll

The output files contain the following information:

- pt_map: integer row and column number of point location in map geometry
- pmap: point location map coordinates (pair of float for Northing / Easting)
- pmapll: point location geographic coordinates (pair of float for latitude / longitude)

9.3. Visualization in map geometry

Using the transformed average backscatter image (in map geometry) displays and rasterfiles can be generated using commands such as:

pdisdt_pwr24_map pt_map pmask3 Luxemburg.utm.dem_par pdef4 1 ave.utm.rmli 0.005 1
prasdt_pwr24_map pt_map pmask3 Luxemburg.utm.dem_par pdef4 1 ave.utm.rmli 0.005 1

A raster image showing a map of the point locations is generated using:

ras_pt pt_map pmask3 ave.utm.rmli.ras pt.utm.ras 1 1 255 0 0 2

and can be displayed using:

disras_dem_par pt.utm.ras Luxemburg.utm.dem_par

which also indicates the coordinates at the point locations.

Deformation histories, together with the point heights, and the quality information can be displayed using vu_disp as follows:

Deformation histories:
vu_disp pt_map pmask3 pSLC_par itab pdisp1 pdef4 phgt4 psigma3 pdh_err3 pdef_err3 pmap pdef4.ras

Examples of screenshots demonstrating this interactive access to the IPTA result are shown below:

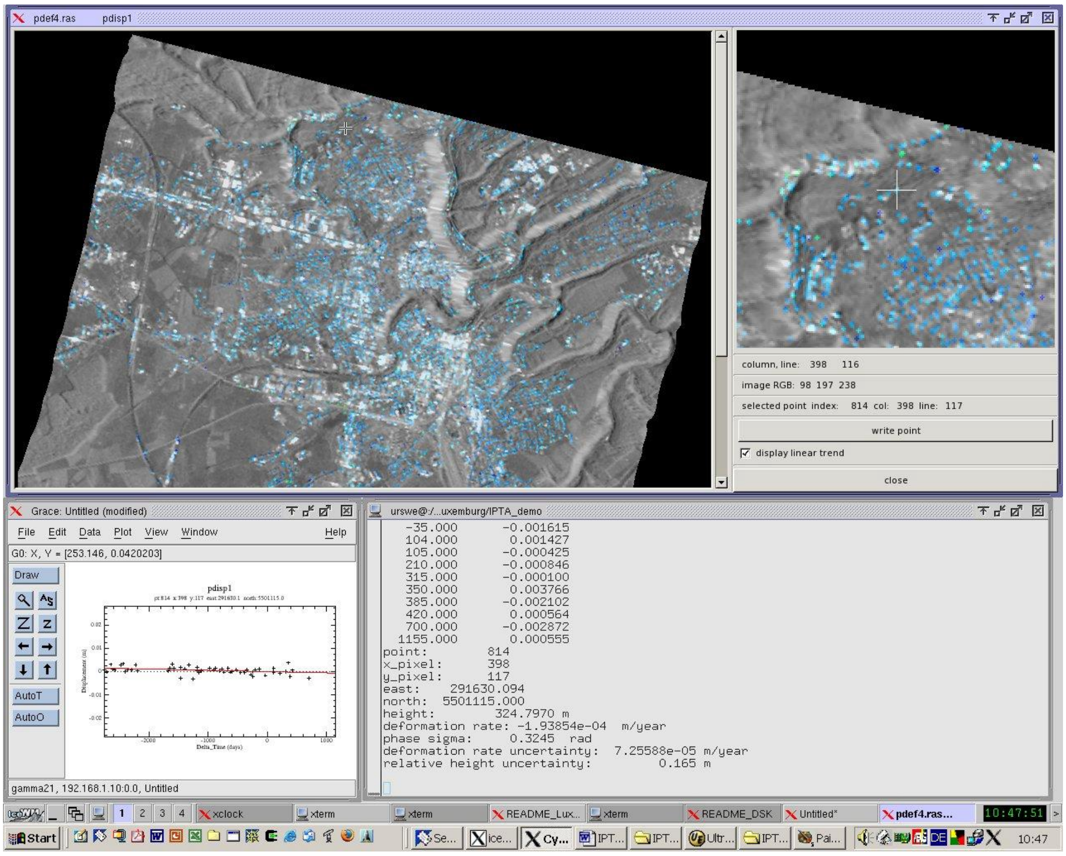

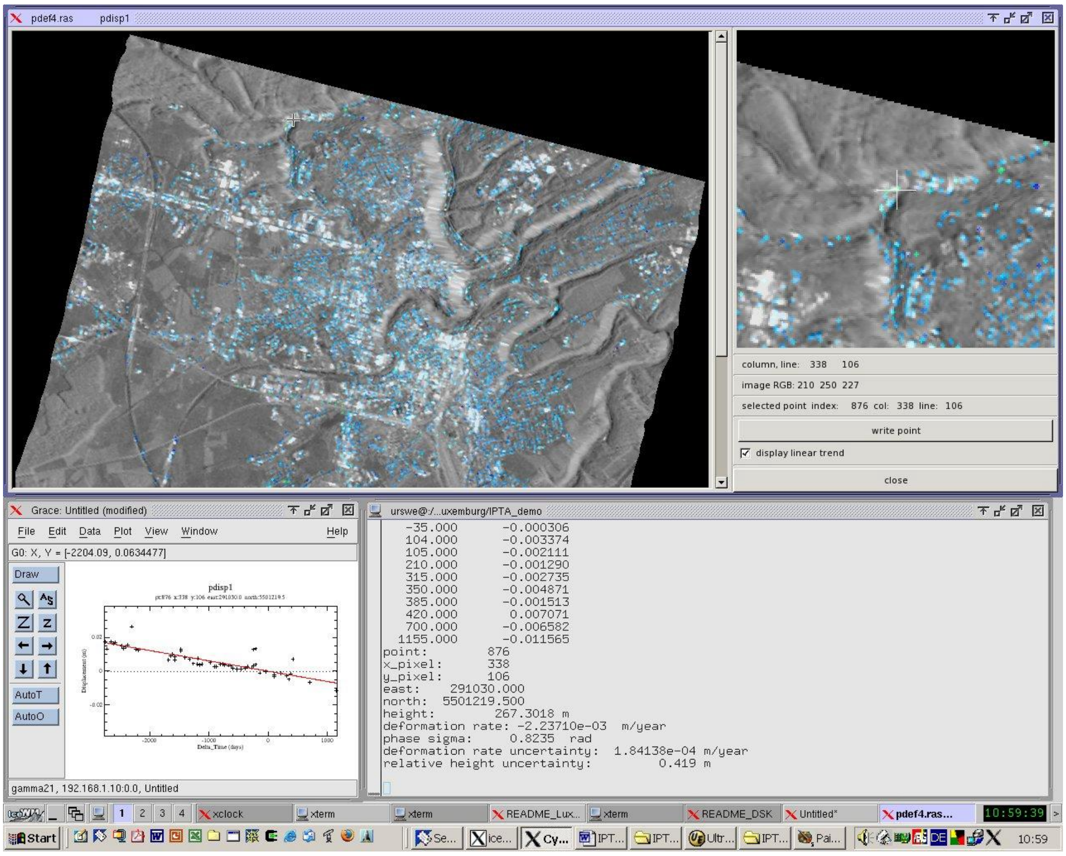

Screenshots demonstrating the interactive access to an IPTA derived deformation history (using vu_disp). A zoom window shows the area around the cursor location at higher resolution. The deformation history of a cursor-selected point is shown in the plot at the bottom left and auxiliary information (coordinates, point height, quality information) for the selected point is indicated in the command shell screen output.

9.4. Reference point coordinates

The reference point coordinate is found using prt_pt:

As SAR and map pixel numbers (col / row):
prt_pt pt pmask3 pt_map 7436 1 8 -
1 7436 216 701 397 354

As map coordinates (in this case UTM; Easting / Northing):
prt_pt pt pmask3 pmap 7436 1 7 -
1 7436 701 216 291620.7812 5498736.0000

And as geographic coordinates (longitude / latitude):

prt_pt pt pmask3 pmapll 7436 1 7 -
1 7436 701 216 6.1158 49.6052

9.5. Deformation time series as ASCII files

ASCII files of results (e.g. as input to GIS) can be generated using the program disp_prt:

disp_prt pt_map pmask3 - pSLC_par itab pmap phgt4 pdef4 psigma3 pdh_err3 pdef_err3 pdisp1 7436 items.txt disp_tab.txt

The two output files, items.txt and disp_tab.txt contain a list of the parameters shown and the data values with one row per accepted point.

Content of file items.txt:

```
  1  point number
  2  x pixel in the reference image
  3  y pixel in the reference image
  4  easting map projection coordinate (m)
  5  northing map projection coordinate (m)
  6  height (m)
  7  deformation rate (mm/y)
  8  standard deviation of the residual phase (rad)
  9  estimated height uncertainty (m)
 10  estimated deformation rate uncertainty (mm/y)
 11  displacement (mm)  date: 1992  4 20  JD: 2448733  days: -2754
 12  displacement (mm)  date: 1992  5 25  JD: 2448768  days: -2719
 13  displacement (mm)  date: 1992  8  3  JD: 2448838  days: -2649
 14  displacement (mm)  date: 1992  9  7  JD: 2448873  days: -2614
 15  displacement (mm)  date: 1992 10 12  JD: 2448908  days: -2579
 16  displacement (mm)  date: 1993  1 25  JD: 2449013  days: -2474
 17  displacement (mm)  date: 1993  3  1  JD: 2449048  days: -2439
 18  displacement (mm)  date: 1993  4  5  JD: 2449083  days: -2404
 19  displacement (mm)  date: 1993  5 10  JD: 2449118  days: -2369
 20  displacement (mm)  date: 1993  7 19  JD: 2449188  days: -2299
 21  displacement (mm)  date: 1993  9 27  JD: 2449258  days: -2229
 22  displacement (mm)  date: 1993 11  1  JD: 2449293  days: -2194
 23  displacement (mm)  date: 1995  3 29  JD: 2449806  days: -1681
 24  displacement (mm)  date: 1995  5  3  JD: 2449841  days: -1646
 25  displacement (mm)  date: 1995  6  7  JD: 2449876  days: -1611
```

```
 26  displacement (mm)  date: 1995  7 12  JD: 2449911  days: -1576
 27  displacement (mm)  date: 1995  7 13  JD: 2449912  days: -1575
 28  displacement (mm)  date: 1995 10 25  JD: 2450016  days: -1471
 29  displacement (mm)  date: 1995 10 26  JD: 2450017  days: -1470
 30  displacement (mm)  date: 1996  1  4  JD: 2450087  days: -1400
 31  displacement (mm)  date: 1996  3 14  JD: 2450157  days: -1330
 32  displacement (mm)  date: 1996  5 22  JD: 2450226  days: -1261
 33  displacement (mm)  date: 1996  7 31  JD: 2450296  days: -1191
 34  displacement (mm)  date: 1996  8  1  JD: 2450297  days: -1190
 35  displacement (mm)  date: 1996  9  5  JD: 2450332  days: -1155
 36  displacement (mm)  date: 1996 10 10  JD: 2450367  days: -1120
 37  displacement (mm)  date: 1997  2 27  JD: 2450507  days: -980
 38  displacement (mm)  date: 1997  5  8  JD: 2450577  days: -910
 39  displacement (mm)  date: 1997  6 12  JD: 2450612  days: -875
 40  displacement (mm)  date: 1997  8 21  JD: 2450682  days: -805
 41  displacement (mm)  date: 1997  9 25  JD: 2450717  days: -770
 42  displacement (mm)  date: 1997 10 30  JD: 2450752  days: -735
 43  displacement (mm)  date: 1998  1  8  JD: 2450822  days: -665
 44  displacement (mm)  date: 1998  2 12  JD: 2450857  days: -630
 45  displacement (mm)  date: 1998  3 19  JD: 2450892  days: -595
 46  displacement (mm)  date: 1998  5 28  JD: 2450962  days: -525
 47  displacement (mm)  date: 1998  8  6  JD: 2451032  days: -455
 48  displacement (mm)  date: 1998 10 15  JD: 2451102  days: -385
 49  displacement (mm)  date: 1998 11 19  JD: 2451137  days: -350
 50  displacement (mm)  date: 1999  1 28  JD: 2451207  days: -280
 51  displacement (mm)  date: 1999  3  3  JD: 2451241  days: -246
 52  displacement (mm)  date: 1999  3  4  JD: 2451242  days: -245
 53  displacement (mm)  date: 1999  4  7  JD: 2451276  days: -211
 54  displacement (mm)  date: 1999  4  8  JD: 2451277  days: -210
 55  displacement (mm)  date: 1999  6 17  JD: 2451347  days: -140
 56  displacement (mm)  date: 1999  9 30  JD: 2451452  days: -35
 57  displacement (mm)  date: 1999 11  4  JD: 2451487  days: 0
 58  displacement (mm)  date: 2000  2 16  JD: 2451591  days: 104
 59  displacement (mm)  date: 2000  2 17  JD: 2451592  days: 105
 60  displacement (mm)  date: 2000  6  1  JD: 2451697  days: 210
 61  displacement (mm)  date: 2000  9 14  JD: 2451802  days: 315
 62  displacement (mm)  date: 2000 10 19  JD: 2451837  days: 350
 63  displacement (mm)  date: 2000 11 23  JD: 2451872  days: 385
 64  displacement (mm)  date: 2000 12 28  JD: 2451907  days: 420
 65  displacement (mm)  date: 2001 10  4  JD: 2452187  days: 700
 66  displacement (mm)  date: 2003  1  2  JD: 2452642  days: 1155

reference point index: 7436
reference point x,y pixel in the reference image: 397  354
reference point easting, northing (m):   291620.781  5498736.000
```

Contents of disp_tab.txt (only the rows for point number 16 and 18 are shown):

```
    16,   525,   101,   292895.406,  5501274.500,   236.117,   -0.589,  0.385, 0.1950,   0.086,   3.733,   4.636,
3.967,   2.375,   3.559,   4.476,   2.867,   2.246,   2.508,   -0.441,   2.806,   1.187,   3.461,   3.874,   4.025,
3.351,   3.358,   2.697,   3.087,   3.400,   2.621,   3.644,   1.155,   1.762,   3.7 79,   2.912,   2.586,   3.463,
3.341,   2.035,   2.059,   1.469,   1.150,   0.546,   2.136,   1.771,   1.537,   2.129,   -0.415,   0.119,   0.209,
1.042,  -0.048,   2.077,   0.160,   5.559,   0.000,  -3.843,   0.471,   0.649,  -1.839,   0.027,  -1.260,  -4.085,
-3.929,                                                                                                    -6.323

    18,   592,   118,   293567.094,  5501098.000,   331.816,   -0.156,  0.468, 0.2360,   0.105,  -1.391,   1.050,
0.655,   0.142,  -0.046,   0.183,   0.132,  -0.523,  -0.477,   0.870,   0.204,   0.056,   8.860,   1.765,   0.620,
1.981,  -0.431,   1.501,   1.552,  -0.098,  -0.570,   1.538,   0.311,   0.276,   0.603,  -0.642,   0.008,   0.148,
-2.433,   0.541,   1.572,   1.660,   1.494,   0.622,   1.595,   1.790,   1.439,   1.848,   2.025,   1.948,   0.770,
```

-2.527, 0.269, -0.079, 1.945, 0.804, 0.000, 1.775, -1.678, -0.782, 0.311, 0.753, 1.495, -1.985, -0.070, -9.654

10. Result files

10.1. ASCII files

items.txt
disp_tab.txt.gz

10.2. Files for interactive visualization using vu_disp

pt_map
pmask3
pSLC_par
itab
pdisp1
pdef4
phgt4
psigma3
pdh_err3
pdef_err3
pmap
pdef4.ras

Command to use:
vu_disp pt_map pmask3 pSLC_par itab pdisp1 pdef4 phgt4 psigma3 pdh_err3 pdef_err3 pmap pdef4.ras